SEDIMENT HARVESTING, BENEFICIAL USE AND THE IMPACT OF CLIMATE AND LAND-USE / LAND-COVER CHANGE ON SEDIMENT LOAD

A Thesis

Presented to

The Graduate Faculty of The University of Akron

In Partial Fulfillment

of the Requirements for the Degree

Master of Science

Richard Owusu Ampomah

August, 2014

SEDIMENT HARVESTING, BENEFICIAL USE AND THE IMPACT OF CLIMATE AND LAND-USE / LAND-COVER CHANGE ON SEDIMENT LOAD

Richard Owusu Ampomah

Thesis

Approved:	Accepted:
Advisor Dr. Lan Zhang	Department Chair Dr. Wieslaw Binienda
Committee Member Dr. Stephen E. Duirk	Dean of the College Dr. George K. Haritos
Committee Member Dr. Christopher C. Miller	Dean of the Graduate School Dr. George R. Newkome
	Date

ABSTRACT

Conventionally, dredged sediment is treated as waste material and disposed in Confined Disposal Facilities (CDFs) or other approved locations. The reason being that sediment gets contaminated as it mixes with finer particles in the range of clay to silt. This range usually contains dissolved contaminants which renders sediment unusable by the EPA and other regulatory standards.

However, new and innovative techniques for harvesting coarser sand and gravel particles using sediment traps is changing the mindset of engineers about dredged sediment. Sediment traps may reduce the flow velocity and allow larger particles to settle making it possible to harvest the desirable portion of the settle-able sediment for beneficial use.

A good knowledge of the total volume and particle size distribution of harvestable sediment is crucial to the design of efficient sediment traps. Hence, there is the need to model and estimate the annual sediment accumulation.

The Ohio Environmental Protection Agency (OEPA) has tentatively agreed for the harvested sediment to be reused directly without remediation Harvesting of sediment in the Cuyahoga River is therefore currently being viewed as a plausible solution to the accumulation of sediment affecting navigation in the Cuyahoga Ship Channel (CSC).

Additionally, the Cuyahoga River Watershed has experienced rapid urbanization over the past two decades. However, few studies have been carried out to assess the impact of this land-use/land-cover (LULC) change on the annual sediment yield.

The study reaches the following conclusions:

(1) On annual average, 71,226 CY (or equivalently 89,513 Ton) of bedload sediment may be harvested from Cuyahoga River with the use of sediment trap. The harvested bedload sediment may be used directly for commercial purpose with the contaminants concentration lower than the EPA standard.

(2) Comparing to the dredging costs, the benefit-cost ratio results in 1.69. The analysis shows harvesting bedload sediment for commercial purpose is more beneficial than dredging the sediments to CDFs.

(3) From the remote sensing analysis, it is found that the developed land area is doubled (23%-47%) in Cuyahoga River watershed above Independence. Additionally, the increasing trend is found for annual precipitation in the watershed. Applying the multiple linear regression analysis, it is found that both LULC and annual precipitation have significant impacts on the suspended sediment yield. One unit increase of annual precipitation contributes more to the sediment yield than the one unit increase of developed land area

ACKNOWLEDGEMENTS

The author's most sincere gratitude goes to my adviser, Dr. Lan Zhang for her guidance, patience and time spent on critiquing my research work and thesis. I would also like to thank my committee members, Dr. Stephen E. Duirk and Dr. Christopher C. Miller who have been a great resource. I am thankful to all other colleagues and friends in the civil engineering department who in diverse ways have contributed to my success at The University of Akron. I am also very grateful of the love and support from my dear wife Dorothy Ampomah and my family throughout my stay at The University of Akron.

TABLE OF CONTENTS

LIST OF TABLES

LIST OF FIGURES

CHAPTER I

INTRODUCTION

1.1 General Overview

The Cleveland Harbor is located on the south shore of Lake Erie and at the mouth of the Cuyahoga River. It is the 7th busiest port in the Great Lakes region and the 51st busiest port in the nation (USACE, 2012). Figure 1.1 shows the location of the Cuyahoga Watershed with 2011 land use and land cover (LULC).

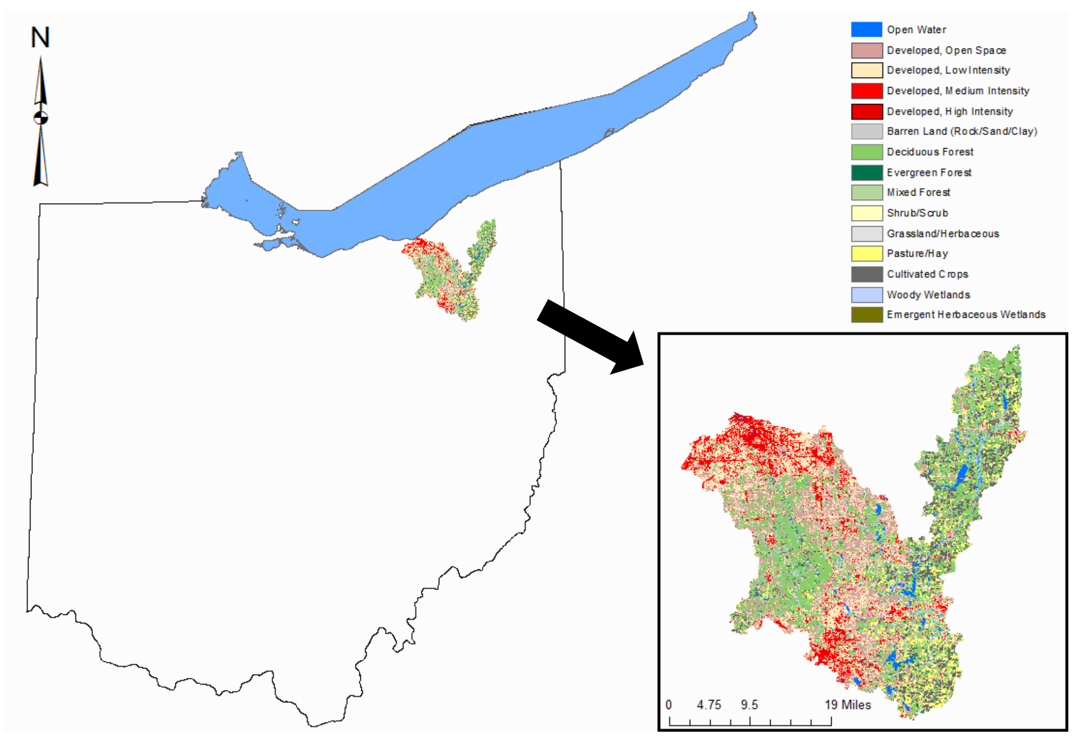

Figure 1. 1: Location Map of the Cuyahoga Watershed

Among 58 federal channels in the Great Lakes region, the Cuyahoga Ship Channel (CSC) is one of the two commercial navigation channels with the highest risk of sedimentation (Kreitinger et al., 2011). Annual dredging has become the common practice to maintain the CSC. Conventionally, the dredged material is disposed in Confined Disposal Facilities (CDFs) (USACE, 2004 ; USACE, 2006 ; Kreitinger, 2011).

Kreitinger, et al. (2011) suggested that annual dredged sediment from the CSC was estimated at 250,000 CY. A new disposal facility or alternative sediment management system needs to be in place by 2015 to sustain the operation of the shipping channel since the capacities of the current CDFs will be exceeded at the end of 2014.

Based on the evaluation of different alternatives (USACE, 2009), the Dredged Material Management Plan (DMMP) for the Cleveland Harbor was drafted to address: (1) plans for dredging maintenance and alternative plans for the disposal of dredged material from CSC; and (2) the impending complete exhaustion of the capacity of CDFs estimated at the end of 2014 (USACE, 2012). However, when the DMMP lost sponsorship in 2009, there was an urgent need for the Buffalo District to pursue an interim measure to enable the maintenance of the channel to meet the minimum federal standards until a substantive plan is in place (USACE, 2012).

Following the in-progress review between the Buffalo District and the Great Lakes and Ohio River Division (LRD), it was agreed to formulate and to obtain the LRD approval for an interim DMMP/EA for 2015 to 2018 (USACE, 2012). This led to several studies including the potential for dredged sediment to be intercepted before reaching the CSC.

This harvested material would then be used for beneficial purposes that might offset some of the cost of dredging and reduce the pressure on CDFs.

Prior to this, few investigations were carried out on the CSC (Hull & Associates Inc ; Moffatt & Nichol, 2012). Recently, a number of studies have focus on investigating the suitability of dredged material for beneficial purposes with the increasing concern about the disposal of dredged sediment from the CSC and the need for a more sustainable alternative to deposition of dredged material in CDFs.

Kreitinger et al., (2011) evaluated the short-term and long-term sediment management options as well as the logistical and technical feasibility of beneficial uses including analysis of the engineering, ecological and environmental suitability and regulatory acceptability. Investigations by Hull & Associates Inc and Moffatt & Nichol (2012) presented more details on sediment transport in the Lower Cuyahoga River system and established the relation between river discharge and sediment rates as well as the proportions of sand and mud in dredged sediment. Their study also discussed the possibility of using sediment traps to intercept sediment before it reaches the CSC.

1.2 Objectives and Scope

The main objectives of this study are: (1) to project the annual harvestable sediment using sediment transport modeling and perform a benefit-cost analysis for harvestable bedload material, and (2) to assess the impact of climate change and LULC changes on suspended sediment load of the Cuyahoga River over the past two decades.

CHAPTER II

LITERATURE REVIEW

2.1 Sediment Transport Modeling

It is well known that there are two main factors governing annual sediment yield: (i) river discharge, i.e., large storms and floods carry most of the sediment annually (Olive and Riger, 1984; Edwards, 1987; Jansson, 1988; Evans, et al, 1997; as few examples), and (ii) underlying surface including the availability of sediment and sedimentary process i.e., consolidation and erosion (Van Leussen, 1991 as an example). In what follows, the /commonly applied sediment transport models are briefly reviewed.

To explain the sediment transport mechanism, Newson, (1986) as well as Webb et al, (1955) stated that sediment transport was dominated by suspended material which may exceed 90% of total sediment transported and generally substantially greater than dissolved material transported (Walling & Webb, 1986).

The TABS-2 and the STUDH models used by USACE in estuarine and riverine sedimentation applies a finite element approach for hydraulic and sediment transport computations (U. S. A. E. Water Experiment Station, 1988). The sediment transport capacity in these two models is determined using Ackers-White total load formula (Ackers and White, 1973). Recent improvements of these models also allow the Modified

Laursen Method (U. S. A. E. Water Experiment Station, 1988) to be applied for sediment transport computations.

Yang C.T. (1989) discussed the basic elements required for sediment transport modeling and fluvial process. He explained the development of a fluvial hydraulic model by combining the stream tube approach, the unit stream power theory and the minimum energy dissipation theory. He also suggested that most hydraulic and sediment routing models were developed mainly to handle subcritical flows such as the well-known HEC-2 and HEC-6.

The Hydrologic Engineers Center's River Analysis System (HEC-RAS) developed based on HEC-2 can perform one-dimensional steady and unsteady hydraulic and sediment transport modeling with mobile bed computations (Brunner, 2010). In HEC-RAS, the hydraulic computation is based on the solution of the one-dimensional energy equation for gradually varied flow and the momentum equation for rapidly varied flow. Manning's equation is employed in energy loss computation together with contraction/expansion coefficients. HEC-RAS computes the sediment transport potential based on grain size distribution and allows for selection from a variety of sediment transport equations and could be used for either single or networked channels. Additionally, similar to the GTSARS4, the HEC-RAS has the capability for simulating cohesive erosion and deposition using the Krone (Krone, 1962) and Partheniades (Partheniades, 1962) methods. The primary assumption in the Krone deposition is that the cohesive material may stick to the bed rather than sink to the bed as sand and gravel. The Parthenaides erosion model is also based on the availability of adequate bed shear against the electrochemical forces holding the grains together.

Lapuszek and Paquier (2008) presented a numerical simulation of sediment transport in mountain rivers using two 1D sediment transport models, i.e., RubarBE and Metoda models, to study bed morphology due to erosion or deposition. This was achieved by analyzing the river bed evolution before training both models. These models relied on the Saint Venant's Equation to govern the flow, the Exner equation for conservation of sediment mass and the Meyer-Peter and Muller sediment transport capacity relation (Meyer-Peter and Muller, 1948).

A review of fluvial processes by Betrie et al. (2011) and Jansen and Bendegon (1979) revealed that sediment is transported either as suspended or bed load depending on particle size and stream flow conditions. They concluded that bed load travels in close proximity with the channel bed whiles suspended sediment moves in the water column above the bed.

Yang and Ahn (2011) developed the GSTARS4 sediment transport model based on GSTARS3 (Yang and Simoes, 2000, 2002) and Sediment and River Hydraulics - One Dimension (SRH -1D) program (Huang and Greimann, 2007). The GSTARS4 model applied the stream tube concept for sediment transport computation which reduced the 3D sediment transport process to semi-2D problem. Hydraulic computations and sediment routing are performed separately for each stream tube. Their study found that using stream tube and the theory of minimum energy dissipation rate (Yang, 1971, 1976; Yang and Song, 1979, 1986) allows for better modeling of the channel morphology.

Griensven et al. (2013) compared the sediment routing of the Simiyu River using the hydrologic model, i.e., Soil and Water Assessment Tool (SWAT) and the 1D hydrodynamic Simulation Software for Rivers and Estuaries (SOBEK-RE) model. The simplified Bagnold's equation (Bagnold, 1977) and well-known Saint Venant equation were applied as governing equations in SWAT and SOBEK-RE model respectively. Similar to other sediment transport models, SOBEK-RE model uses different sediment transport equations depending on particle size distribution (Griensven et al., 2013). In their study, they found that most of the sediment load formula, e.g., Ackers and White bed and suspended load formula (Ackers and White, 1973), the Engelund and Hansen total load equation (Engelund and Hansen, 1967), the Meyer- Peter bed load formula (Mayer-Peter, 1984), the Parker and Klingeman bed load formula (Parker and Klingeman, 1982), and the van Rijn bed and suspended load formula (van Rijn, 1984), are all applicable sediment transport functions.

Bever and MacWilliams (2013) quantified the spatial and temporal variability of sediment concentration in San Pablo Bay using a three dimensional hydrodynamic, wind wave and sediment transport model of San Francisco Bay and Sacramento-San Joaquin Delta with the underlying principle: once the bed shear stress exceeds the sediment's critical shear stress for erosion, sediment is suspended from the seabed and transported by ambient currents (Miller and Komar, 1973; Hill and McCave, 2001). By combining 3D UnTRIM San Francisco Bay-Delta Model (Casulli and Zanolli, 2002, 2005) with

Simulating Waves Nearshore (SWAN) wave model (SWAN Team, 2009) and the SediMorph morphological model, their study showed that the proposed model could reasonably predict hydrodynamics, waves and suspended sediment concentration in San Pablo Bay.

Fernandez-Nieto et al. (2014) introduced a new approach to evaluating bedload transport flux suited for sediment transport in shallow water regimes. Their approach comprised of dividing the sediment into two layers: the top layer that moves as a result of river hydraulics and bottom layer which does not move but is susceptible to move. Dividing the sediment into two layers allowed sediment mass to be better preserved and resulted in more realistic results.

2.2 Impact of Climate and LULC Change on Sediment Load

Population growth and urban developments within the watershed may have many negative consequences on water resources. Notable among them are the effects on flooding, erosion and water quality. Human activities such as the construction of roads, buildings, and parking lots result in the loss of pervious land surfaces. The loss of pervious land surface considerably reduces the infiltration thereby increasing the total runoff amount generated by a given rainfall event. Additionally, natural erosion rate may be accelerated by construction, agriculture, mining, and tree felling in the watershed. As a result, the accelerated erosion rate may increase the sediment supply to surface water (Nelson and Booth, 2002).

Additionally, according to the Intergovernmental Panel on Climate Change (IPCC, 2007), the earth's climate is changing due to increased emission of greenhouse gases. Higher sea levels, intense storms and heavy rainfall events are some of the likely effects of the constantly changing climate (McBean and Ajibade, 2009). Therefore, a good understanding of the contribution of climate change and human activities serves as a scientific basis for future land and river ecological management (Wang et al., 2012). In what follows, the impacts of climate and LULC change to sediment yield are briefly reviewed.

Nelson and Booth (2002) studied how human activities changed predevelopment sediment transport rates. To reveal the impact of human activities, they developed the watershed-scale sediment budget for an urbanizing watershed through the evaluation of significant sources, quantities and delivery of sediment. They found that the human activities were responsible for nearly 50% of the change in annual sediment yield.

Dearing and Jones (2003) reviewed lake sediment-based studies in which sediment flux patterns and the impact of land use and climate were investigated. They concluded that the impact of land-use on sediment flux for smaller catchments ($<10^3$ km^2) is much bigger than that of climate change. They also reported an increase in the magnitude of sedimentation flux of about five to ten times of the pre-disturbance rates.

Odhiambo and Boss (2006) compared the importance of watershed physiography and LULC on sediment yield and reservoir sedimentation in the Lee Creek Reservoir and Lake Shepherd Springs. They found that watersheds within the same climate zone and geological formation may result in different yields due to other contributing factors such as the physiographic properties, especially slope.

Van Dessel et al. (2008) assessed the impact of potential land cover change on mean annual sediment using stochastic allocation algorithms and flow algorithms. They achieved this by first downscaling regional land cover scenarios to the landscape scale using stochastic algorithms. Then, they evaluated the impact of expected changes on mean annual sediment. They concluded that sediment delivery to the lake was expected to increase due to a relation between sediment sources and sinks within the catchment.

Rose et al. (2011) studied the impact of land use on sediment rates in lowland regions. They also reported an increasing pattern of sedimentation rates over the second half of the 20th century similar to the results found by Schiefer et al. (2013) who studied lake sediment deposits in western Canada.

Thothong et al. (2011) assessed the impact of land use change and rainfall on sediment and carbon accumulation for a reservoir of North Thailand. They classified precipitation into erosive and non-erosive using 10mm as the threshold and employed Landsat 5TM and 7TM satellite imagery and ENVI 4 (Canty, 2007) software to classify the land cover into three classes using the maximum likelihood supervised classification (Lillesand and Keiger, 2008) and corroborated with the use of the field survey. Their study indicated that fine sediment transported in suspension was linearly related to erosive rainfall, while the bedload sediment accumulation did not respond linearly to extreme rainfall events.

Wang et al. (2012) investigated the effects of climate change and human activities on annual streamflow. Their approach involved using a Pettitt mutation method to detect trends any changes in annual streamflow for the period between 1961 and 2008. Then they applied SWAT model to separate different effects from climate change and human activities. Finally, they independently estimated the impacts of climate change and human activities on streamflow with the use of sensitivity-based method and simulation method respectively. Their study showed that the impacts of human activities on streamflow accounted for over 50% and concluded that human activities were the main factors affecting streamflow and sediment flow into the Hoa Binh Reservoir.

Schiefer et al. (2013) related temporal trends of sediment accumulation to the patterns of land use and climate change for lake catchments using linear mixed effect design. Their study revealed an increasing trend in sediment accumulation with land use change, i.e., increase of the urban development. Although climate change also had an impact on sediment accumulation, its effect was relatively small compared to that of land use change.

The above studies indicated the negative impacts of climate and LULC change to sediment yield, i.e., the climate and LULC change have the potential to increase the sediment yield. However, it must be it is must be mentioned that there are some human activities which could decrease the sediment yield considerably (Walling, 1999). As an example, five major dams on the Missouri River reduced sediment yield at its mouth by more than 50% between 1950s and 1980s (Meade and Parker, 1984), due to the sediment being trapped by the dam.

Besides the combined impact of climate and LULC change on total sediment yield, it is also a great concern to engineers, scienties and ecologists with the following reasons: (1) continuous deposition of coarse sediment in channels causes bed aggradation resulting in reduced flow capacity that may cause flooding or affect navigability of channel (Nelson and Booth, 2002) (2) fine sediment is also a major source of water-quality problems as they form complexes with clay minerals hence causing lake eutrophication and toxicity to aquatic organisms (Nelson and Booth, 2002 ; Novotny and Olem, 1994).

Historically, for CSC, the study has been mainly focused on the impact of sediment to the navigation and corresponding dredging management. Few studies have been carried out on the impacts of climate change and LULC change in the Cuyahoga Watershed. Therefore, it is very important to investigate the impact of climate and LULC change in the watershed as it provides a scientific basis for future land and river ecological management.

CHAPTER III

METHODOLOGY

This chapter explains the governing equations, data, methods, and assumptions applied in the study. The first part of the chapter focuses on sediment transport modeling and benefit cost analysis of harvested bedload sediment. The second part focuses on explaining the LULC change detection and a Multiple Linear Regression (MLR) of suspended sediment load on annual change of LULC and precipitation.

3.1 Sediment Transport Modeling and Benefit Cost Analysis

HEC-RAS is applied to study the sediment transport. HEC-Geo-RAS is applied to construct the geometry file of the study region. The sediment transport model includes two components: the hydraulic model and the sediment transport simulation. In what follows, the hydraulic model and sediment transport simulation are discussed in detail.

3.1.1 Governing Equations for Hydraulic Computations

The Hydraulic Model involved water surface profile computations using the energy equation and the Standard Step Method (Brunner, 2010; Methods et al., 2003).

This involves balancing the energy equation using an iterative process suggested by Henderson (1966). Figure 3.1 is a representation of the energy equation.

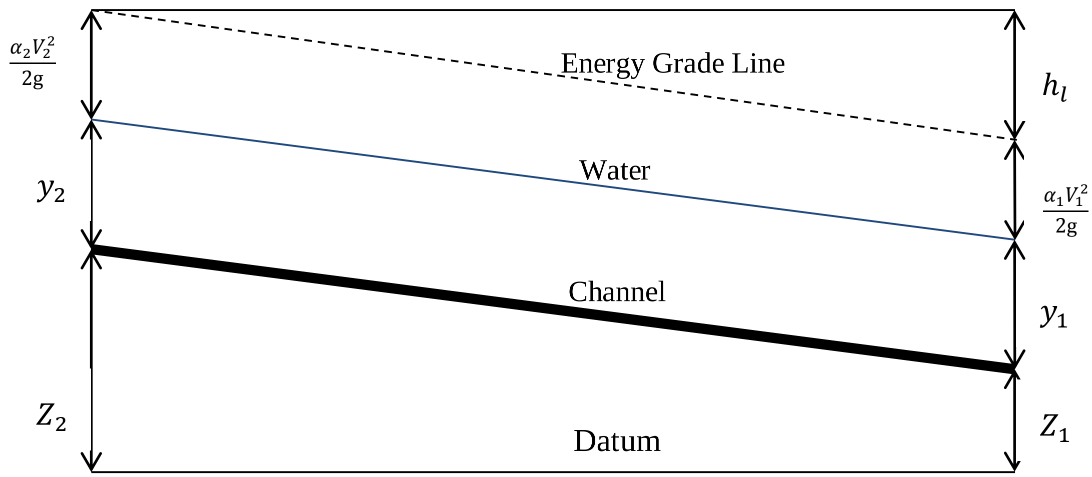

Figure 3. 1: Representation of the Energy Equation

Equation (3.1) represents the energy equation depicted in Figure 3.1 as:

$$Z_2 + y_2 + \frac{\alpha_2 V_2^2}{2g} = Z_1 + y_1 + \frac{\alpha_1 V_1^2}{2g} + h_l \tag{3.1}$$

where Z is bed elevation; y is the water depth; V is velocity; α is velocity distribution coefficient; and h_l is total head loss.

Henderson (1966) proposed an iterative procedure based on the Newton-Raphson root finding method. According to this iterative method, if the energy equation is represented as a function of the water surface elevation (WSEL), the root of the function may be found using Equation (3.2) as:

$$WSEL_{improved} = WSEL_{initial} - \frac{f(WSEL_{initial})}{f'(WSEL_{initial})} \tag{3.2}$$

where $WSEL_{initial}$ is the initial guess for the water surface elevation and $WSEL_{improved}$ is improved water surface elevation after each iteration.

Now, based on Figure 3.1, the total energy at cross section 2 may be represented in two different ways as:

$$H_{21} = Z_2 + y_2 + \frac{V_2^2}{2g} \tag{3.3}$$

$$H_{22} = H_1 + \frac{1}{2}\Delta x\left(S_{f_1} - S_{f_2}\right) \tag{3.4}$$

where H_{21} is the total head at cross section 2 expressed as a function of potential head, pressure head and kinetic head. H_{22} is the total head at cross section 2 expressed as a function of total head at cross section 1 , friction slope S_f and distance Δx between two cross sections.

Assuming ΔH as the difference between the two heads H_{21} and H_{22}, the objective is to minimize ΔH to an acceptable tolerance using:

$$\Delta H = H_{21} - H_{22} = Z_2 + y_2 + \frac{V_2^2}{2g} - H_1 + \frac{1}{2}\Delta x S_{f_1} - \frac{1}{2}\Delta x S_{f_2} \tag{3.5}$$

Now, given $\Delta H = H_{21} - H_{22}$ and $WSEL = z + y$, Equation (3.2) can be rewritten as

$$WSEL_{improved} = WSEL_{initial} - \frac{\Delta H}{\frac{d(\Delta H)}{dy_2}} \tag{3.6}$$

The denominator in Equation (3.6) can be further simplified as:

$$\frac{d(\Delta H)}{dy_2} = \frac{d}{dy_2}\left(y_2 + \frac{V_2^2}{2\mathrm{g}} - \frac{1}{2}\Delta x S_{f_2}\right) \tag{3.7}$$

To solve Equation (3.7), it may be simplified with the following two assumptions (Henderson, 1966): (1) for a natural channel, the top width approximately equals the wetted perimeter, and (2) friction slope S_f varies approximately as the inverse cube of the flow depth (y). Therefore, Equation (3.7) is reduced to:

$$\frac{d(\Delta H)}{dy_2} = 1 - Fr_2^2 + \frac{3S_{f_2}\Delta x}{2R_2} \tag{3.8}$$

where Fr is the Froude number, Δx is the distance between the two cross sections, S_f is the friction slope and R is the hydraulic radius.

Substituting Equation (3.8) into Equation (3.6), one obtains:

$$WSEL_{improved} = WSEL_{initial} - \frac{\Delta H}{1 - Fr_2^2 + \frac{3S_{f_2}\Delta x}{2R_2}} \tag{3.9}$$

Considering Eddy losses = $\frac{1}{2}C_L\left(\frac{V_1^2}{2\mathrm{g}} + \frac{V_2^2}{2\mathrm{g}}\right)$ by multiplying Fr_2^2 in Equation (3.9) by a factor of $\left(1 - \frac{1}{2}C_L\right)$, Equation (3.9) is rewritten as:

$$WSEL_{improved} = WSEL_{initial} - \frac{\Delta H}{1 - Fr_2^2\left(1 - \frac{1}{2}C_L\right) + \frac{3S_{f_2}\Delta x}{2R_2}} \tag{3.10}$$

where C_L is the coefficient of expansion or contraction. C_L is taken as 0.1 for contraction and 0.3 for expansion.

Equation (3.10) provides an improved guess of water surface elevation to be used in the next iteration. The iteration ends when the difference between $WSEL_{improved}$ and $WSEL_{initial}$ is within a predefined acceptable tolerance.

A hydraulic jump is considered when flow transits from a supercritical to a subcritical regime. In this case, the momentum equation is applied for the water surface profile computation as:

$$\frac{Q\gamma}{\mathrm{g}}(\beta_2 V_2 - \beta_1 V_1) = P_1 - P_2 + \mathrm{Wsin\theta} - F_f \tag{3.11}$$

where γ is unit weight of water; β = momentum coefficient; P is pressure at cross section; W is weight of water enclosed between cross sections; F_f is total friction force acting along the channel boundary; V is the velocity at the given cross section; and θ is the angle of inclination of the channel bed.

Assuming θ is very small; Equation (3.11) is simplified as:

$$\frac{Q^2}{A_1\mathrm{g}} + A_1\bar{y}_1 = \frac{Q^2}{A_2\mathrm{g}} + A_2\bar{y}_2 \tag{3.12}$$

where $\bar{y}$ is depth to centroid of cross section from the water surface; A is the cross sectional area and Q is the discharge. For a discretized natural cross section, $\bar{y}$ is obtained as:

$$\bar{y} = \frac{\sum_{i=1}^{n} A_i \, \bar{y}_i}{A} \tag{3.13}$$

where n is the number of sub cross sections. A trial and error method may then be used to find the sequent depths before and after the hydraulic jumps.

3.1.2 Hydraulic Computations Procedure

Water surface profile is computed by first determining the normal and critical depths at all cross-sections. The normal and critical depths are then compared to ascertain the flow regime, i.e, subcritical, supercritical or critical (Brunner, 2010). Additionally, water surface profile is computed in the upstream direction for subcritical reaches and in the downstream direction for super critical reaches (Molinas and Yang, 1985).

Normal depth is computed using:

$$\mathrm{g}(y) = Q - K(y)\sqrt{S} = 0 \tag{3.14}$$

where y is flow depth; $K(y)$ is conveyance ; S is bed slope; and Q is discharge.

Critical depth is computed using:

$$f(y) = 1 - \alpha(y)\frac{Q^2 T(y)}{\mathrm{g}A^3(y)} = 0 \tag{3.15}$$

where α is velocity distribution coefficient; $T(y)$ is top width of cross section; and $\mathrm{A}(y)$ is cross sectional area.

The main assumption implemented by HEC-RAS to model the sediment transport is to approximate the hydrograph with a quasi-unsteady state hydrograph. The discharge, in this case, remained constant over each computation time step as shown in Figure 3.2. The quasi-unsteady flow modeling provides an easier, faster and simpler way of combining hydraulic computations and sediment transport as opposed to a more complex and computationally expensive unsteady state sediment transport (Brunner, 2010).

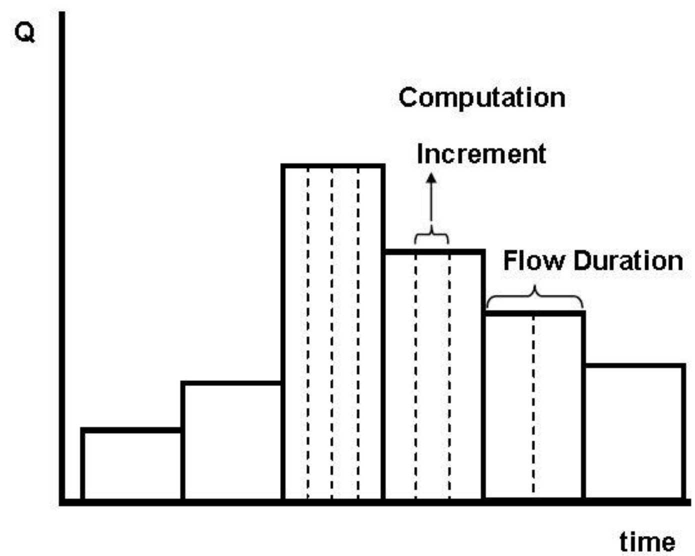

Figure 3. 2: Quasi-Unsteady Hydrograph (Brunner, 2010)

In this study, the flow duration used in the quasi-unsteady flow analysis is 24 hours. Therefore, discharge value remains constant over the computation increment of 24 hours. The same time step was applied to the temperature and sediment time series.

3.1.3 Boundary Conditions for Hydraulic Computations

Figure 3.3 shows the location of the four control stations applied in the sediment transport model. The downstream boundary (Newburgh Heights) is set a discharge-stage rating curve. The upstream boundary (Harim Rapids) is a hydrograph of daily mean discharge obtained from USGS.

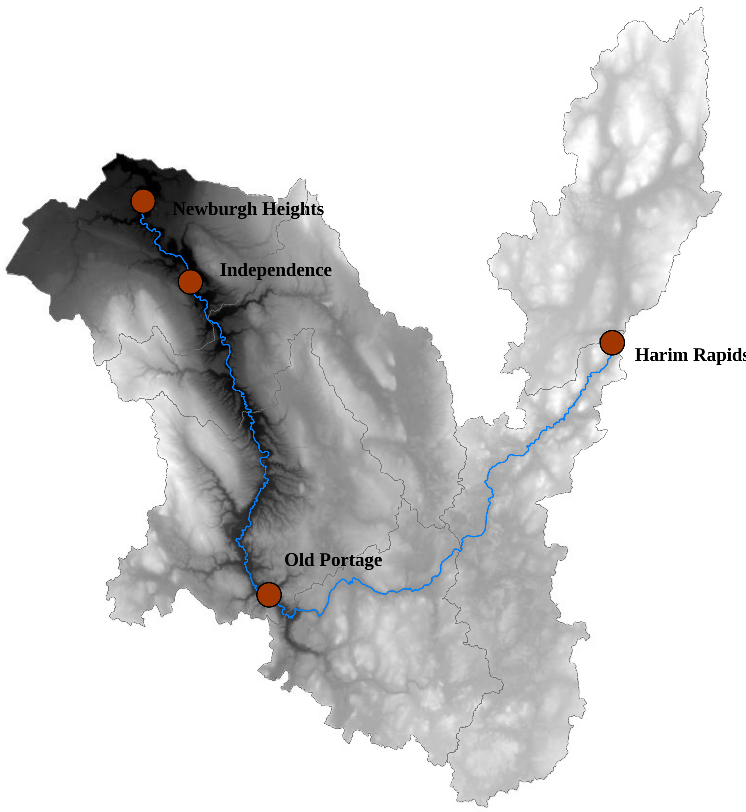

Figure 3. 3: Cuyahoga Watershed with Gage Stations

For the downstream boundary condition at Newburgh Heights, the computed discharge-stage rating curve is applied instead of the measured discharge–stage relation published by USGS due to the following two reasons: (1) there is approximately 70ft elevation difference between the DEM and the USGS datum; (2) there is a lined concrete canal that is not depicted by the USGS DEM. The lined concrete canal is about 150ft wide and begins approximately 800ft upstream of Newburgh Heights. Thus, with this knowledge, the discharge rating curve is built with the use of the Manning's Equation:

$$Q = \frac{1.49}{n} R^{2/3} S^{1/2} A \tag{3.16}$$

where Q is the discharge, n is the manning's roughness coefficient, S is the bed slope, R is the hydraulic radius and A=bh is the cross-sectional area with b and h as bottom width and flow depth for rectangular channel respectively.

Since the surface width of the channel is much bigger than the flow depth, one may assume that the hydraulic radius R is approximately equal to the flow depth (h). Then Equation (3.16) is simplified as:

$$Q = \frac{1.49}{n} h^{5/3} S^{1/2} b \tag{3.17}$$

Using the average bed slope S =$5.67\text{x}10^{-5}$ computed from DTM and manning's roughness coefficient for concrete of 0.017, Equation (3.17) is rewritten as:

$$h = \left[\frac{Q}{15.75}\right]^{3/5} \tag{3.18}$$

Figure 3.4 shows the rating curve obtained for Newburg Heights after the modification.

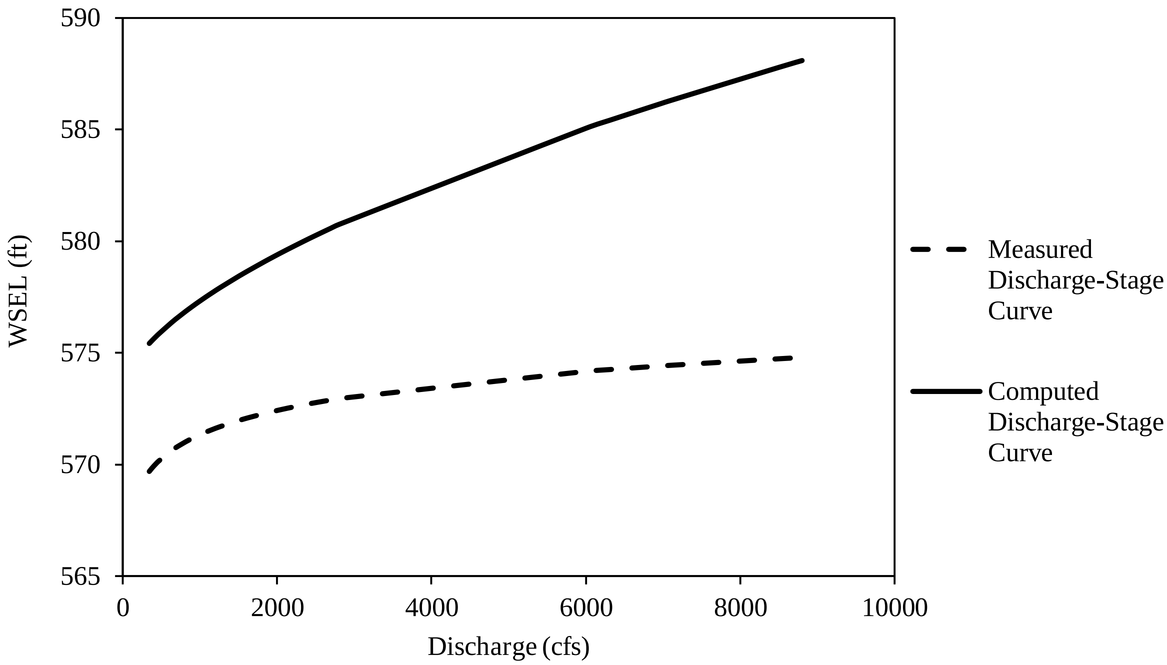

Figure 3. 4: Comparison of Discharge - Stage Curves at Newburg Heights

Sediment transport computation is composed of two parts. The sediment transport capacity is computed first followed by the bed elevation change computations. The sediment transport capacity is computed as a fraction of the transport potential computed with one of seven transport functions available in the model.

3.1.4 Sediment Transport Capacity Computation

The Ackers-White transport function is selected to compute transport potential based on particle size distribution of channel bed, average bed slope, average velocity and temperature range (Appendix A). The Ackers-White transport potential computation procedure is explained following Brunner (2010) as:

For a given particle size range of median diameterd_{si}, the dimensionless grain diameter d_{gr} is given as:

$$d_{gr} = d_{si}\left[\frac{g.(s-1)}{v^2}\right]^{\frac{1}{3}} \tag{3.19}$$

where s is specific gravity, v is kinematic viscosity; and g is the gravitational acceleration.

The sediment mobility number is given as:

$$F_{gr} = \frac{{u_*}^n}{\sqrt{g d_{gr}(s-1)}}\left[\frac{V}{\sqrt{32}log\left(\alpha\frac{D}{d_{si}}\right)}\right]^{1-n} \tag{3.20}$$

where $u_* = \sqrt{g.D.S}$, D is the flow depth , g is the gravitational acceleration, S is bed slope, V is the velocity, α is a constant usually assumed as 10 (Brunner, 2010), d_{gr} is dimensionless grain diameter , d_{si} is median particle diameter , s is specific gravity and n is the sediment size-related transition exponent given as:

$$n = \begin{cases} 1 \text{ if } d_{gr} \leq 1 \\ \left(1 - .056\log\left(d_{gr}\right)\right) \text{ if } 1 < d_{gr} \leq 60 \\ 0 \text{ if } d_{gr} > 60 \end{cases} \tag{3.21}$$

The sediment transport parameter G_{gr} is given as:

$$G_{gr} = C\left(\frac{F_{gr}}{A} - 1\right)^m \tag{3.22}$$

where A , C, F_{gr} and m are defined as follows:

The initial motion parameter (A) is given as:

$$A = \begin{cases} \left(\frac{0.23}{\sqrt{d_{\mathrm{gr}}}} + 0.14\right) \text{ if } d_{gr} \leq 60 \\ 0.17 \text{ if } d_{\mathrm{gr}} > 60 \end{cases} \tag{3.23}$$

The sediment transport function coefficient (C) is given as:

$$C = \begin{cases} 10^{2.79.log(d_{\mathrm{gr}}) - 0.98[\log(d_{\mathrm{gr}})]^2 - 3.46} \text{ if } d_{\mathrm{gr}} \leq 60 \\ 0.025 \text{ if } d_{\mathrm{gr}} > 60 \end{cases} \tag{3.24}$$

And the sediment transport function exponent (m) is computed as:

$$m = \begin{cases} \left(\frac{6.83}{d_{\mathrm{gr}}}\right) \text{ if } d_{\mathrm{gr}} \leq 60 \\ 1.78 > 60 \end{cases} \tag{3.25}$$

The sediment flux is then computed as:

$$X = \frac{G_{\mathrm{gr}} s d_{si}}{D\left(\frac{u_*}{V}\right)^n} \tag{3.26}$$

where s is specific gravity; d_{si} is median particle diameter; D is flow depth; u_* is shear velocity; V is velocity; n is size-related transition exponent; and G_{gr} is sediment transport parameter.

Finally, the Transport Potential (T_p) for each grain class is computed by:

$$T_p = \gamma_w Q X \tag{3.27}$$

where γ_w is the unit weight of water; Q is the discharge; and X is the sediment flux.

According to Einstein (1950), sediment discharge for a given grain size is proportional to the fractional abundance of that class. Based on this assumption, a representative transport value known as transport capacity is computed, i.e., the transport capacity T_c as:

$$T_c = \sum_{k=1}^{n} P_k T_{p_k} \tag{3.28}$$

where T_{p_k} is the transport potential and P_k is the percentage of the active layer that the grain class represents.

3.1.5 Bed Elevation Change Computation

The one dimensional sediment transport model is governed by the sediment continuity equation as:

$$\frac{\partial Q_s}{\partial x} + \eta \frac{\partial A_d}{\partial t} + \frac{\partial A_s}{\partial t} - q_{lat} = 0 \tag{3.29}$$

where $\eta = 1 - \text{porosity}\,(\lambda_p)$; A_d is the volume of bed sediment per unit length; A_s is volume of sediment in suspension at the cross section per unit length; Q_s is volumetric sediment discharge; and q_{lat} is lateral sediment inflow.

Following Wu and Wang (2006), the porosity is defined as:

$$\lambda_{\mathrm{p}} = 0.245 + \frac{0.0864}{(0.1d_{50})^{0.21}} \tag{3.30}$$

where λ_{p} is the porosity of sediment deposit; and d_{50} is the median diameter of sediment mixture in millimeters.

Assuming the change in suspended sediment concentration at any cross section is much smaller than the change of the river bed as

$$\frac{\partial A_s}{\partial t} \ll \eta \frac{\partial A_d}{\partial t} \tag{3.31}$$

Equation (3.29) can be rewritten as:

$$\eta \frac{\partial A_d}{\partial t} + \frac{\partial Q_s}{\partial x} = q_{lat} \tag{3.32}$$

To solve equation (3.32) numerically, the finite difference numerical scheme is applied to approximate $\frac{\partial A_d}{\partial t}$ as:

$$\frac{\partial A_d}{\partial t} \approx \frac{\Delta A_d}{\Delta t} \approx \frac{(aT_{i-1} + bT_i + cT_{i+1})\Delta Z_i}{\Delta t} \tag{3.33}$$

where T is the top width; Z is the change in bed elevation; i is the cross section index; and a, b and c are constants such that $a + b + c = 1$.

Similarly, $\frac{\partial Q_s}{\partial x}$ in Equation (3.33) can be approximated as:

$$\frac{\partial Q_s}{\partial x} = \frac{\Delta Q_s}{\Delta x} = \frac{Q_{s,i} - Q_{s,i-1}}{1/2\,(\Delta x_i + \Delta x_{i-1})} \tag{3.34}$$

Substituting Equations (3.33) and (3.34) into Equation (3.32), one obtains:

$$\eta_i \; \frac{(aT_{i-1} + bT_i + cT_{i+1})\Delta Z_i}{\Delta t} + \frac{Q_{s,i} - Q_{s,i-1}}{1/2\,(\Delta x_i + \Delta x_{i-1})} = q_{lat} \tag{3.35}$$

To this end, the change of bed elevation due to each sediment size fraction may be solved numerically as:

$$\Delta Z_{i,k} = \frac{\Delta t}{\eta_i} \frac{q_{lat}(\Delta x_i + \Delta x_{i-1}) + 2(Q_{s,i-1,k} - Q_{s,i,k})}{(aT_{i-1} + bT_i + cT_{i+1})(\Delta x_i + \Delta x_{i-1})} \tag{3.36}$$

where k is size fraction index; η_i is volume of sediment in a unit bed layer at cross section i; $Q_{s,i,k}$ is computed sediment transport potential, and T_{p_k} is transport potential per unit length for size class k.

The total bed elevation change at each cross-section i is then computed as an aggregation of the bed change for individual classes using:

$$\Delta Z_i = \sum_{k=1}^{N} \Delta Z_{i,k} \tag{3.37}$$

3.1.6 Model Data and Representation

The overall objective of the simulation is to estimate annual sediment accumulation using the historical hydrologic information. Therefore, the simulation is performed with the 10-year historical records. The computed average result for these 10years was then considered as an annual result.

Daily mean streamflow (cfs) for each station are obtained from USGS and the National Center for Water Quality Research at the Heidelberg University (NCWQR). Four discharge stations are used in this study: the Cuyahoga River at Hiram Rapids OH (04202000), Cuyahoga River at Old Portage OH (04206000), Cuyahoga River at Independence OH (04208000) and Cuyahoga River at Newburgh Heights OH (04208504). Appendices G, H and I shows the hydrographs at Independence, Old Portage and Harim Rapids Respectively.

The Southerly Wastewater Treatment Plant (S.W.T.P) in Cuyahoga Heights which contributes an approximate average of 125mgd (232cfs) and a peak of 400mgd (743cfs) to the Cuyahoga River (North Ohio Regional Sewer District, 2014) is modeled as the tributary of the Cuyahoga River at Cuyahoga Heights.

A Digital Elevation Model (DEM) published by USGS National Map Viewer (2011) is used to represent the Cuyahoga River. Horizontal datum of DEM is the North American Datum 1983 (NAD83). Vertical Datum is the North American Vertical Datum of 1988 (NAVD88) (U.S Geological Survery, 2009). The Ohio State Plain is used for DEM projection.

Suspended sediment information forms an important part of the model. An equilibrium boundary condition is set for the uppermost cross section, i.e., Hiram Rapids due to lack of the suspended sediment information. With this assumption, the computed sediment transport capacity at that cross-section is used as the sediment inflow rate for each time step of the reach (Brunner, 2010 ;Yang, 1989). The observed sediment hydrograph at Independence (Appendix J) is applied as the control location.

The computation of sediment transport capacity and transport potential is dependent on the particle sizes available for transport both in suspension and as bed load. Kreitinger et al. (2011) carried out surface grab sampling in the Cuyahoga River in 2010 for eight locations. The closest to the Independence station is adopted as suspended sediment gradation. Figure 3.5 shows the suspended sediment particle gradation used for the model.

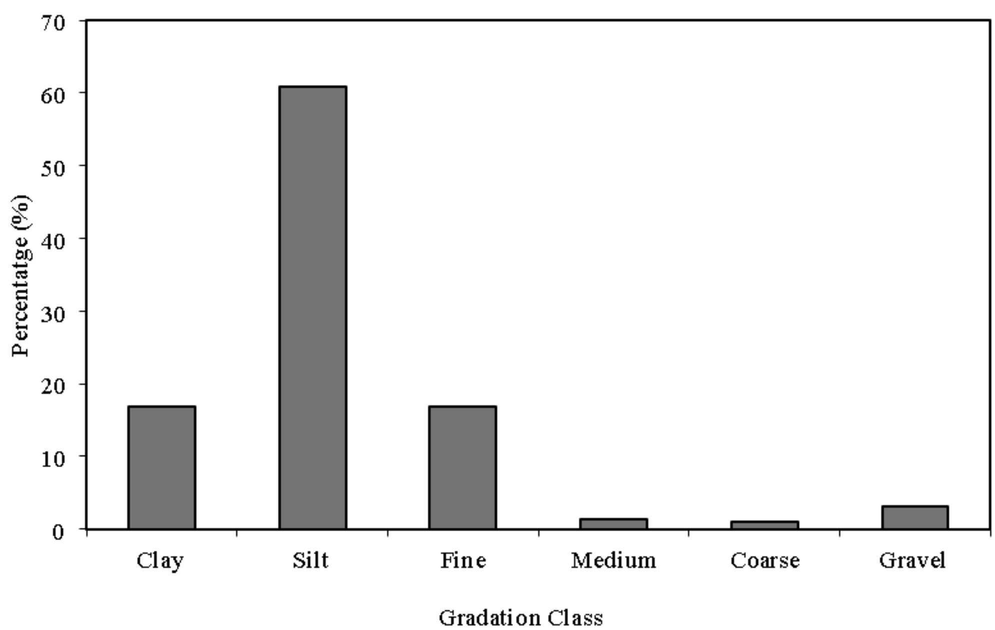

Figure 3. 5: Suspended Sediment Gradation (Kreitinger et al., 2011)

The effect of temperature is also considered in the model. Tang et al. (2012) discussed the importance of temperature on streamflow by different seasons of the water year. Mean water temperature and the kinematic viscosity are related as:

$$\upsilon = \frac{1.792 \text{ x } 10^{-6}}{1.0 + 0.0337T + 0.000221T^2} \tag{3.38}$$

where υ is kinematic viscosity; and T is the temperature in degree centigrade.

And the kinematic viscosity is related to the fall velocity (Rubey, 1933) as:

$$\omega = \mathrm{F}_1\sqrt{(\mathrm{s}-1)\mathrm{g}d_{si}} \qquad \text{where} \quad \mathrm{F}_1 = \sqrt{\frac{2}{3} + \frac{36\upsilon^2}{\mathrm{g}d_{si}^3(\mathrm{s}-1)}} - \sqrt{\frac{36\upsilon^2}{\mathrm{g}d_{si}^3(\mathrm{s}-1)}} \tag{3.39}$$

where g is the gravitational acceleration, d_{si} median particle size and s is the specific gravity.

Temperature information for the Cuyahoga River is obtained from the Independence gage station. Assuming a similar climate across the entire watershed, the temperature at Independence is applied for modeling the entire channel.

Sieve analysis was conducted on bedload samples at ArcelorMittal, Big Creek/Bradley Road and Mill Creek (Duirk and Gnap, 2013). 100g of air-dried soil sample was tested using sieve numbers 4, 6, 8,10,30,50,100 and 200. Following different calibrations of the model with the various samples and their composites, the Bradley Road sample is found to produce the most acceptable result shown in Figure 3.6.

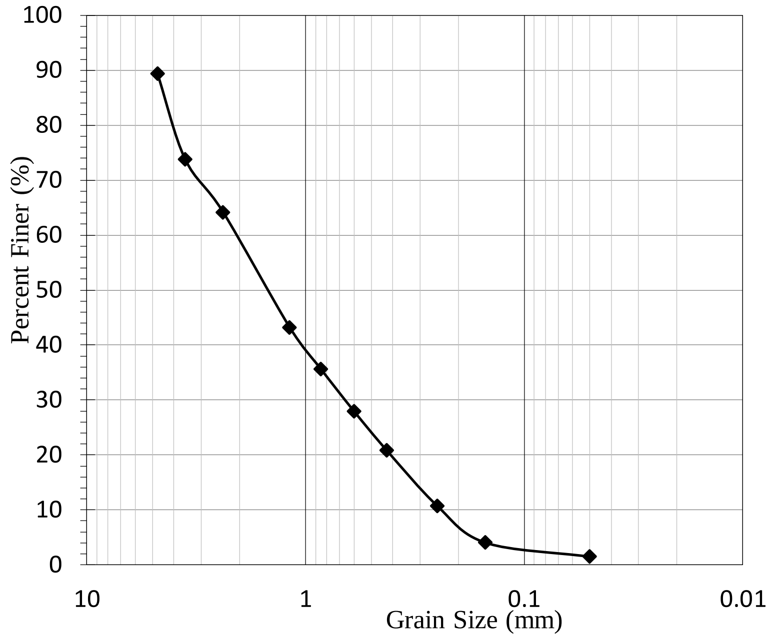

Figure 3. 6: Bed Gradation at Bradley Road

Then, the sediment transport computation is carried out using a representative grain size for each grain class. This grain size is computed as the geometric mean of the grain class (Brunner, 2010) based on the American Geophysical Union classification (Appendix B).

The assumption in the choice of the manning's roughness coefficient is that the channel is a natural channel except for the last 800ft to Newburgh heights which is a concrete lined channel. Manning's coefficients are selected according to cross section classification as overbanks or channel. 0.070 and 0.030 are selected as the Manning's coefficient for overbank and channel respectively while 0.017 is selected for concrete-lined canal.

According to Parker (1991), as erosion occurs over time, a layer of coarse material is formed which limits supply of sediment. This layer, i.e., the amor layer, leads to a preferential transport of finer grain material which explains the decrease in the characteristic grain size in the downstream direction for most gravel rivers.

Taking armor layer into consideration , the Exner 5 sorting and amoring method (Thomas, 1982) is employed. This method subdivides the active layer into a cover and subsurface layer with the cover layer being the only layer actively involved in the erosion or deposition process (Brunner, 2010).

3.1.7 Harvesting Sediment with Sediment Trap

Sediment traps or interceptors have been used successfully in several drainage systems to prevent clogging from debris. In river systems, a sediment trap retains sediment being transported from upstream. This helps maintain dredging requirements in navigation channels. According to USEPA (2012), sediment traps may efficiently capture sand while allowing the clay and fine silt to pass.

The mechanism of sediment trap is based on the inverse proportionality between velocity (V) and cross sectional area (A) i.e. $V \propto \frac{1}{A}$. By increasing the depth at a given cross section, the velocity decreases which allows the coarser particles to settle in the sediment trap as illustrated in Figure 3.7. The efficiency of sediment traps depends on the intensity of rainfall, erosion and proper maintenance (USEPA, 2006). Average sediment trap efficiency is estimated at 60 percent by (USEPA, 1993, USEPA, 2006) and up to 75 percent (Smolen et al., 1998).

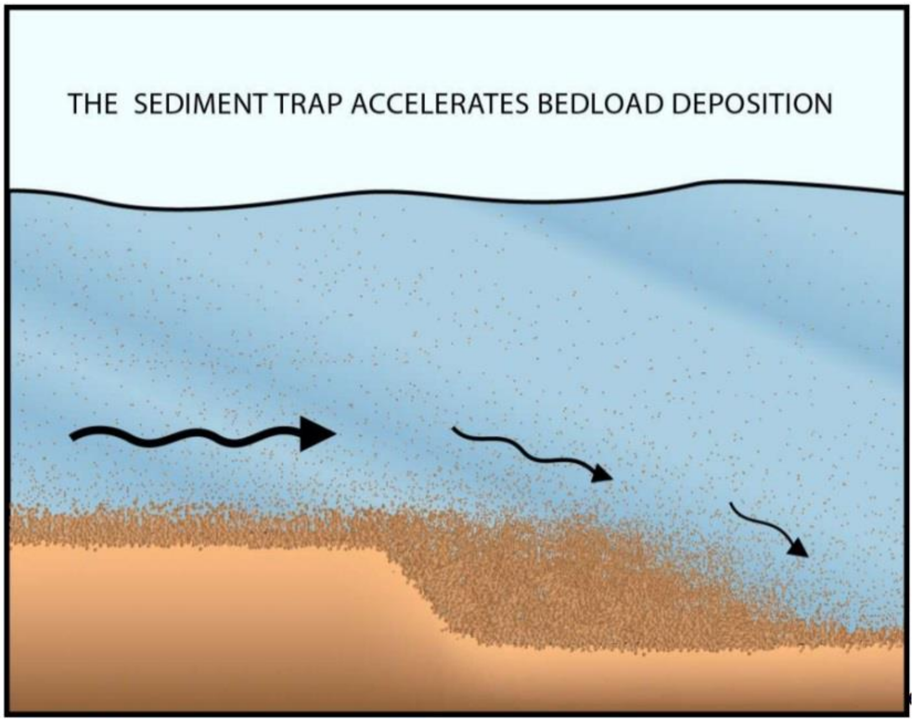

Figure 3. 7: Sediment Trap (USEPA,2012)

Bearing these limitations in mind, the monthly harvestable bedload is estimated by multiplying the monthly bedload by an efficiency coefficient listed in Table 3.1 chosen according to the streamflow classification based on the comparison of the 10 year monthly mean discharge with the historical (30year) monthly mean discharge listed in Table 3.2.

Table 3. 1: Efficiency Coefficients for Computing Harvestable Bedload

	Efficiency Coefficients	
Flow Classification	CS-FG	VFS-MS
High flow	0.6	0.15
Low flow	0.75	0.3

Appendix K shows a comparison of the average shear velocities with the particle fall velocities of the various particle sizes

Table 3. 2: Monthly Streamflow Classification

Month	Flow		Classification
	30-year Mean (cfs)	10-year Mean (cfs)	
JAN	1272.681	1153.6	Low
FEB	1476.571	2706.31	High
MAR	1691.077	1149.27	Low
APR	1509.294	848.837	Low
MAY	1150.168	847.049	Low
JUN	836.1742	484.081	Low
JUL	672.5516	380.391	Low
AUG	523.3065	250.076	Low
SEP	583.0065	689.756	High
OCT	616.8581	368.79	Low
NOV	930.6548	1228.32	High
DEC	1279.119	1229.92	Low

3.1.8 Benefit Cost Analysis

Potential beneficial use options identified by Kreitinger et al. (2011) include mine land reclamation, littoral nourishment, wetlands/habitat creation and landfill cover. According to Duirk and Gnap (2013), most of the organic and inorganic contaminants in the sediment are below OEPA allowable concentrations. Therefore, havested sediment may also be used as construction material.

3.1.8.1 Market Value of Harvestable Sediment

Mason sand particle size ranges from 0.60mm (#30 Sieve) to 0.15mm (#100 Sieve) whiles concrete sand particle ranges from 2.0mm (#10 Sieve) to 0.3mm (#50 Sieve) (Premier Equastrian, 2013). These two types of material fall within the range (0.125mm to

8mm) of harvestable bedload. Medium Sand (MS) - Very fine sand (VFS) portion of the harvested bedload may be used as masonry sand whiles the Coarse Sand (CS) - Fine Gravel (FG) may be used for concrete sand. Table 3.3 summarizes a review of market value for mason and concrete sand from five sources.

Table 3. 3:Summary of Market Value of Construction Sand

	Market Value	
Source	Mason Sand ($)/ton	Concrete Sand ($)/ton
Westhook Sand& Gravel (2014)	29	19.5
Area Mulch &Soil (2014)	34	-
Kirbysand (2014)	25	-
Wenatchee Sand&Gravel (2014)	23.55	17.55
Acmesand (2014)	-	21.63
Average	27.89	19.56

3.1.8.2 Cost of Dredging to CDFs

Identified cost components of dredging to CDFs as shown in Table 3.4 includes estate acquisition (right of way), site preparation, transportation to site, material handling, transportation to end user, and permitting & regulatory cost (Kreitinger et al., 2011).

Table 3. 4: Dredging Cost (Kreitinger et al., 2011)

	Dredging Method	
Cost Item	Mechanical Dredging to CDF $/ CY	Hydraulic Dredging to CDF $/ CY
Dredging	7.65	11.17
Estate Acquisition/Right of Way	0	0
Site Preparation	2.27	0.73
Transportation to Handling Site	0	4.03
Transportation to End User	9.2	10.2
Material Handling Drying	4.02	5.73
Permitting & Regulatory Cost	0.38	0.38
Total Cost	23.52	32.24

3.2 Modeling the Impact of Climate and LULC Change on Suspend Sediment Load (SSL)

According to the discussion of the impact of climate and LULC change on sediment load in CHAPTER I, LULC change and precipitation within Cuyahoga watershed of 21years is applied to study their impacts on suspended sediment load. Multiple Linear Regression (MLR) is applied to evaluate the impacts of climate and LULC change on the annual suspended sediment load. Figure 3.8 shows the study area with discharge gage station at Independence , the weather station at Akron-Canton, Ravena, Chippewa,Harim and Chardon, and areas where majority of LULC occurred in the past 21 years, i.e., upstream of Independence.

Total Annual precipitation data at the Akron-Canton, Ravena, Chippewa, Harim and Chardon is collected from the National Oceanic and Atmospheric Administration (NOAA) for the period of 1991 to 2011. Appendix F shows the thiessen weighted average precipitation computed from the four weather stations. Annual mean suspended sediment loading is obtained from the Independence gage station. Figures 3.9 and 3.10 show an increasing trend in the both the total annual precipitation and annual mean suspended sediment load for the 21 years studied.

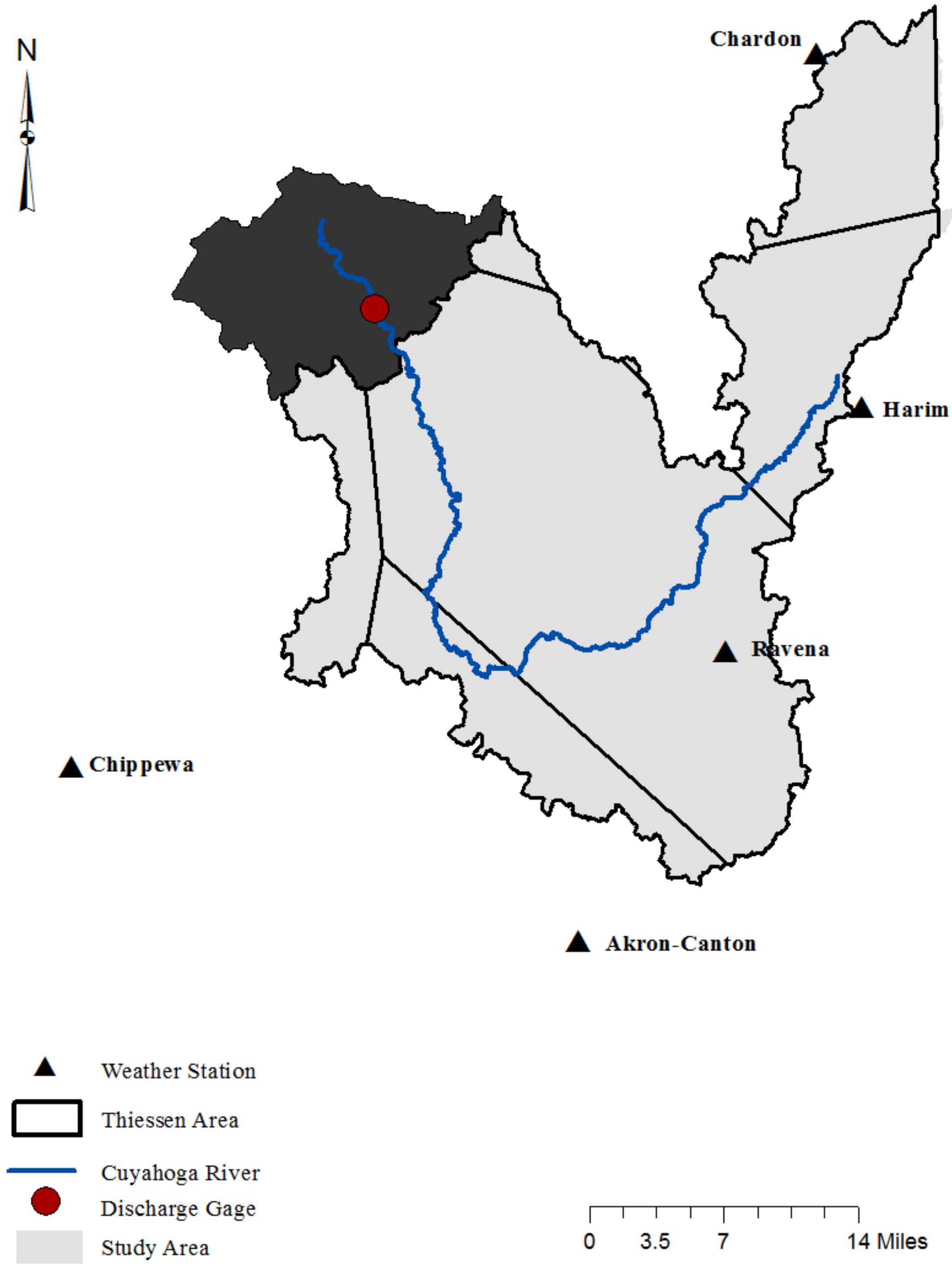

Figure 3. 8: Study Area with Gage Station Locations

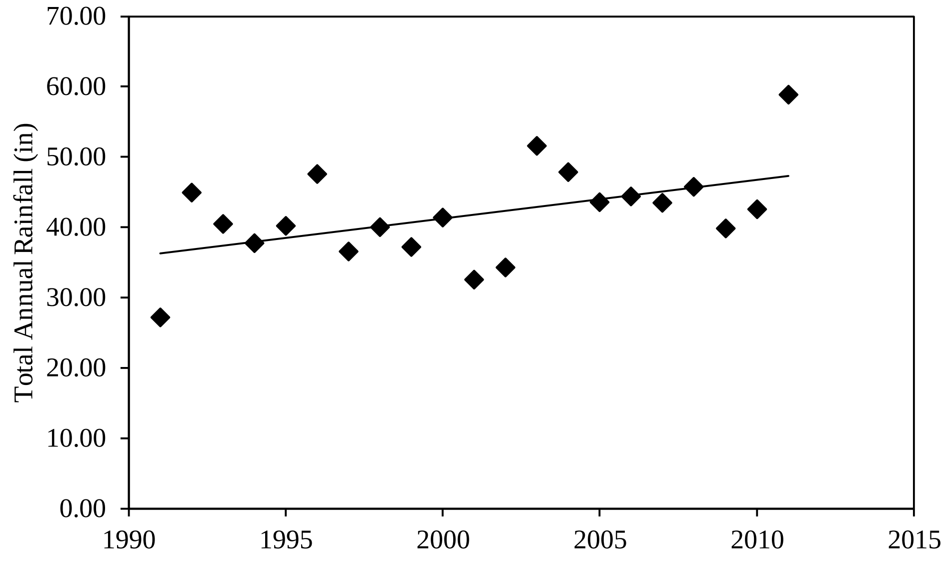

Figure 3. 9: Total Annual Precipitation

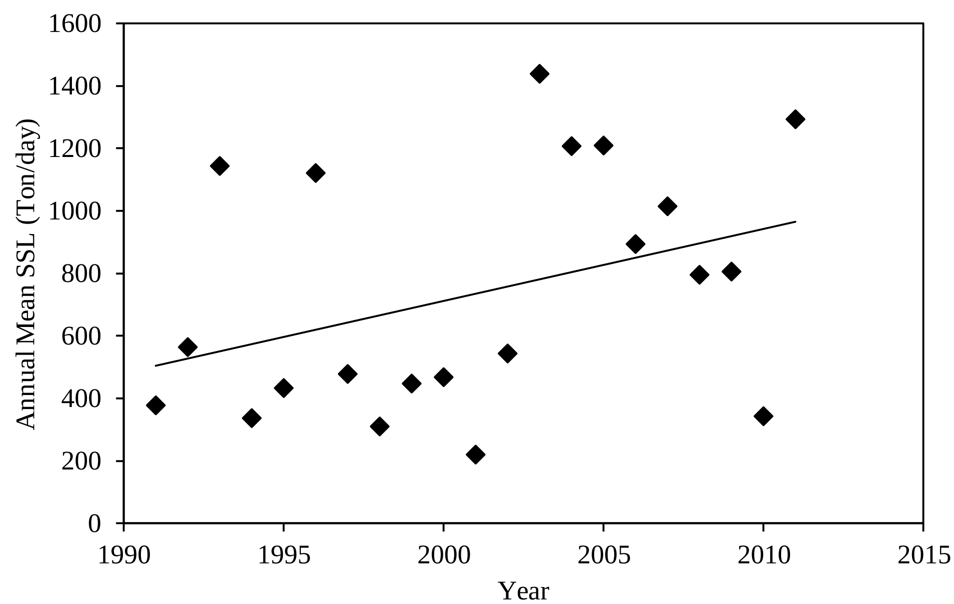

Figure 3. 10: Annual Mean Suspended Sediment Load (SSL)

3.2.1 LULC Change Detection with Remote Sensing

LULC change of the Cuyahoga watershed is studied using satellite images obtained between 1991 and 2011. Remote sensing analysis is based on the ENVI 5.1 model and ArcGIS 10. The Cuyahoga watershed falls within the World Reference System (WRS) row/path 18/31 and 18/32 (USGS, 2013). Satellite images from the Landsat 5 program are obtained from the USGS Global Visualization Viewer (USGS GLOVIS) for these two scenes. The images used are standard terrain corrected (level 1T) images which are radiometrically and geometrically corrected (USGS, 2013).

Images for the analyses are taken between April and September of each year to minimize the effect of clouds. For images in which clouds could not be avoided (example in Appendix C), a masking technique was used which will be further explained.

The satellite images are first calibrated for spectral reflectance. This allows subsequent image to be analyzed using the actual percentage of reflected sunlight (0-100%) instead of brightness of the pixels (0-255) (Jensen, 2005). Next, a dark object subtraction is performed to correct for atmospheric scattering of light (noise) by subtracting the minimum spectral reflectance value from each pixel in the entire image (Jensen, 2005). A mosaic of the pair of images for each year, WRS 18/31 and WRS 18/32 is then cropped using the Cuyahoga watershed as an outline.

The classification scheme applied in this study consisted of three classes: (1) developed land including rooftops, roads, pavements, parking lots and other impervious land cover types; (2) undeveloped land including agricultural land, forests, bare soil and other pervious land cover types; and (3) open water including lakes, rivers and all other water bodies.

Supervised classification is applied as the classification method. Training samples are developed using National Land Cover Dataset (NLCD) images from 1992, 2001 and 2006 as the reference images. A minimum of 50 training samples are developed for each class which are collected at locations where no changes in land cover occurred between 1991 and 2011. Following minimum distance algorithm for image classification (Jensen, 2005), the distances between each pixel value and the means of three classes are compared and each pixel classified under the class whose mean is closest to that pixel value (Jensen, 2005). Figure 3.11 illustrates image processing and classification of the 1991 image.

Unavoidable clouds in images are classified separately. The clouded area is then compared with the images of the immediate years before and after to detect LULC change

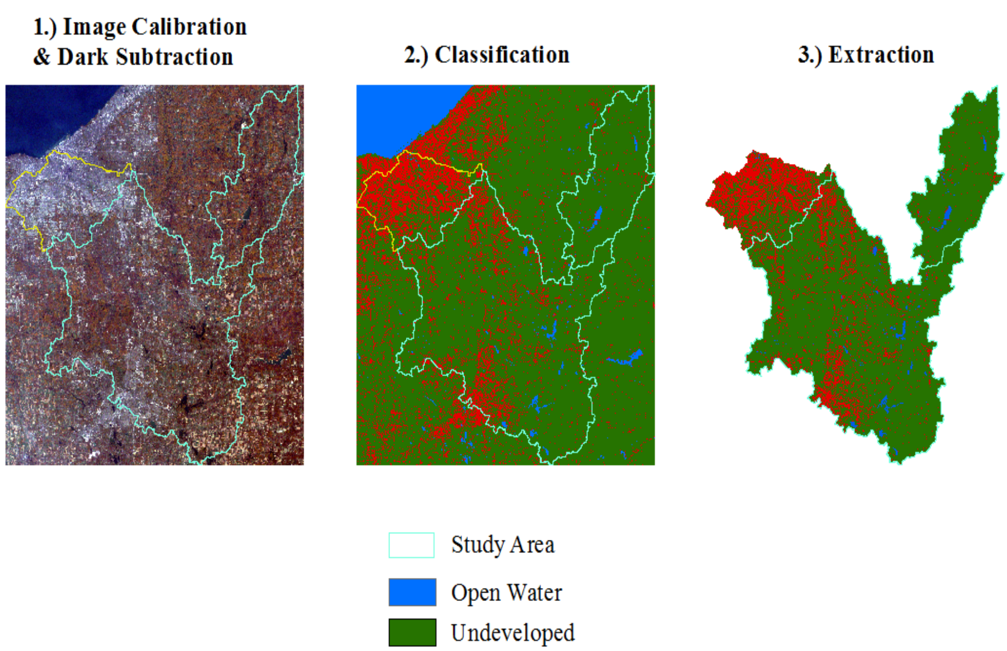

Figure 3. 11: Image Processing and Classification

within the two periods. The affected pixels are then masked depending on whether the change occurred. Appendix D and E show an example of the images before and after masking.

3.2.2 Multiple Linear Regression

Multiple linear regression model is applied to predict the suspended sediment load and to study the impacts of climate and LULC change on suspended sediment load. Using annual precipitation and LULC as independent variables, the expected suspended sediment load is given as:

$$E(SSL|PRCP, LULC) = \alpha + \beta_1 PRCP + \beta_2 LULC \tag{3.40}$$

where $E(SSL|PRCP, LULC)$ is the expected value of the suspended sediment load given the predictors PRCP and LULC; α, β are the intercept and slopes of the fitted MLR model.

CHAPTER IV

RESULTS AND DISCUSSION

The first part of this chapter discusses the results from sediment transport model and benefit cost analysis of harvested sediment using the proposed sediment trap. The simulated average sediment accumulation result for 10-year period is compared with annual dredged sediment volumes reported by Kreitinger et al. (2011) to assess the accuracy of the model.

The second part of the chapter interprets the results of a predictive model regarding to the assessment of the impact of climate change and LULC change on the suspended sediment load of the Cuyahoga channel. The predicted results are then compared with the observed annual mean suspended sediment to assess the accuracy of the model.

4.1 Bedload Estimate, Characterization and Benefit Cost Analysis Result

The average cumulative monthly bedload estimated from 10-year result is illustrated by Figure 4.1. According to the bedload particle sizes, the predicted bedload is grouped into Clay and Silt (0.002mm-0.008mm), Very Fine Sand (VFS) to Medium Sand (MS) (0.0625mm-0.5mm) and Coarse Sand (CS) to Fine Gravel (FG) (0.5mm-8mm).

The predicted total sediment accumaltion was 414,009.53CY or 407,441.19Tons (Figure 4.1)

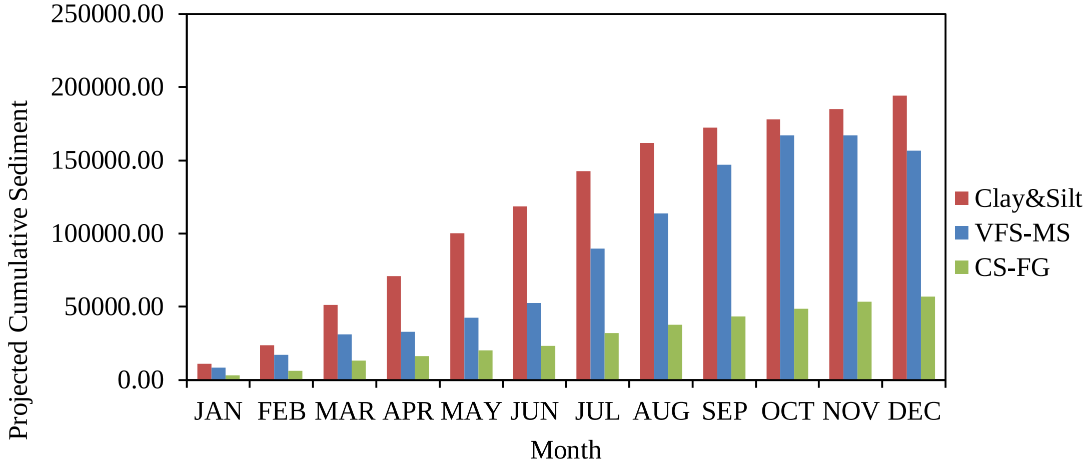

4.1: Projected Cumulative Monthly Sediment for 10-year's Averaged Result

Table 4.2 illustrates the cumulative harvestable bedload computed by applying sediment trap efficiency coefficients (Table 3.1) discussed in CHAPTER III to the cumulative monthly sediment results in Figure 4.1. Total annual harvestable bedload is then predicted as 71,226.01 CY or 89,513.77 Ton.

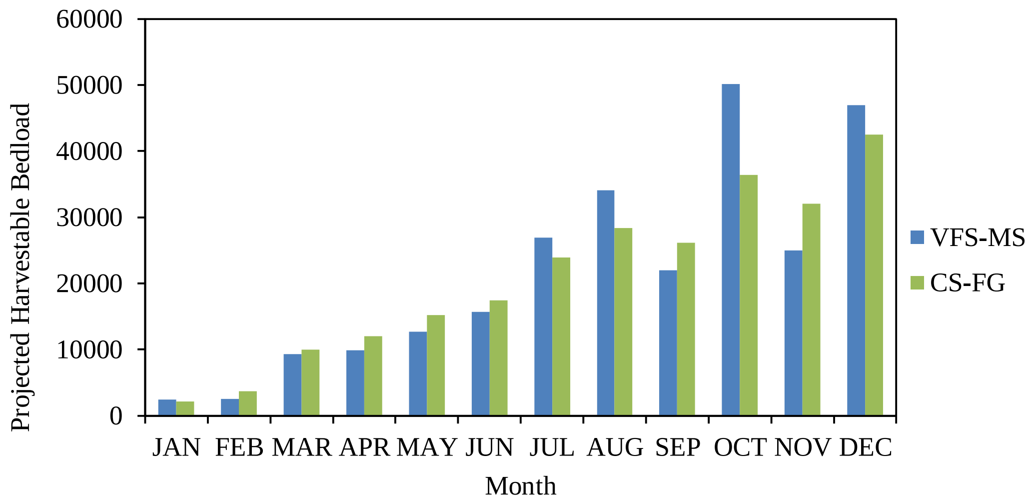

4.2: Projected Harvestable Bedload

Table 4.1 lists the comparison between the model projected sediment (414,009.53 CY) and actual annual dredged volumes of 295,000 CY, and 225,000 CY for 2002 and 2007 respectively as reported by (Kreitinger et. al, 2011). Considering the fact that the CSC is not dredged to its fully autorized depth of 23ft (Hull & Associates Inc ; Moffatt & Nichol, 2012), a prediction of 414,009.53 CY is well within range of annual sediment accumulation at Newburgh Heights.. The higher percentage of gravel from model results may be explained by the fact that the channel is not dredged to its full depth. The Possible overestimation may be due to the following reasons: (1) dams, bridges and other hydraulic structures were not modeled in this study due to the limitation of available information; (2) incompatibility of DTM with the USGS datum at Newburg Heights such that the discharge rating curve needs to be revised as the boundary condition; and (3) measurement error.

Table 4. 1: Comparison of Model Results with Dredged Annual Volumes

	Dredged in 2002		Dredged in 2007		Model 10-Year Average	
Material	CY Removed	Percentage (%)	CY Removed	Percentage (%)	CY Projected	Percentage (%)
Clay&Silt	236,550	80.19	143,255	63.67	244,777.06	59.12
Sand	51,100	17.32	79,875	35.50	124,607.43	30.10
Gravel	6,350	2.15	55	0.02	45,125.05	10.90
Total	295,000	99.66	225,000	99.19	414,009.53	100

4.1.1 Cost of Sediment Dredging to CDFs

The historical average annual dredged volume is estimated at 250,000 CY (Kreitinger, et al., 2011). Based on this estimate, the capitalized annual costs for mechanical and hydraulic dredging to CDF were estimated as follows:

Capitalized Cost = A/I.

where A is annual dredging cost; and I is the interest rate.

According to the unit costs of both mechanical and hydraulic dredging to CDFs discused in CHAPTER III (Table 3.4) and the Ohio Department of Taxation (2014), the annual interest rate for 2014 is 3% . Then the capitalized costs of mechanical and hydraulic dredging to CDF are computed as:

Capitalized Cost of Mechanical Dredging to CDF = Annual Unit Cost/interest(I)

= \$23.52/ CY/0.03

= \$784 /CY

Capitalized Cost of Hydraulic Dredging to CDF = Annual Unit Cost/interest(I)

= \$32.2/CY/0.03

= \$1074 /CY

4.1.2 Construction and Maintenance Cost of Sediment Trap

The estimated installation cost of the bedload interceptor in the Cuyahoga River is \$1,000,000. It includes equipment installation, automation and engineering cost. The annual operation and maintenance (O&M) cost (approximately \$5/CY) includes electricity and maintenance of the bedload interceptor, pump maintenance as well as labor and maintenance of front and end loader. Using the estimated harvestable bedload of 71,226.01CY (Table 4.2), the installation cost per cubic yard of harvestable sediment is \$1,000,000/71,226.01CY = \$14.15/CY. Then the final total capitalized cost is given as:

Total capitalized cost = (Installation Cost + Capitalized Annual O&M cost)/I

= (\$14.15/CY +\$5/CY)/0.03

= \$638.33/CY

Table 4.2 summarizes the total annual harvestable sediment. By applying limiations of the sediment trap with the use of efficiency coefficients, the total annual harvestable sediment is estimated as 71,226.01CY (89,513.77Ton) including 46,980.37CY (37,382.23Ton) very fine sand (VFS) to medium sand (MS) and 42,533.40CY (33,843.78Ton) coarse sand(CS) to find gravel(FG).

Table 4. 2: Summary of Annual Harvestable Sediment

	VFS-MS		CS-FG		Total	
	Ton	CY	Ton	CY	Ton	CY
Total Annual	46,980.37	37,382.23	42,533.4	33,843.78	89,513.77	71,226.01

Using the harvestable very fine to medium sand as mason sand (\$27.89/ton) and harvestable coarse sand to fine gravel as concrete sand (\$19.56/ton), Table 4.3 summarizes the projected total annual benefit. And in general, the benefit per cubic yard of the harvestable sediment results in \$2,142,235.82/66,092CY = \$32.41/CY.

Table 4. 3: Projected Annual Amount from Harvested Sediment

Material	Projected Annual Harvestable (ton)	Average Market Value ($/ton)	Projected Annual Amount from construction material ($)
Mason Sand	46,980.37	27.89	1,310,282.52
Concrete Sand	42,533.40	19.56	831,953.30
		Total	**2,142,235.82**

Considering the annual benefit of $32.41/CY as perpetuity, the present value is then computed as:

Present Value (Capitalized benefit) = Perpetuity /Interest Rate.

= $32.41/CY/0.03

= $1080.43/CY

Following Miche (2001), the benefit cost analysis is studied with use of the four step method as: (1) forecasting the annual benefits (B) and costs (C), (2) determining the discount rate, (3) computing the Net Present Value (NPV), and (4) comparing the alternatives to ensure $\mathrm{B}-\mathrm{C} \geq 0$ or $\mathrm{B}/\mathrm{C} \geq 1$.

Benefit-Cost Ratio = Present Value of Annual Benefits/ Capitalized cost

= $1080.43/$638.33/CY = 1.69

A benefit cost ratio greater than 1 indicates profitability (Miche, 2001). Thus it is beneficial to utilize the harvestable sediments for commercial use.

4.2 Impacts of Climate and LULC Change on Suspended Sediment Load (SSL)

The LULC change is studied using remote sensing satellite imagery. The available Land Cover images (1992, 2001, and 2006) published by USGS are applied as the control images for the identification of LULC change. Additionally, interpolation method is applied when the image is either unavailable or could not be processed due to excessive cloud or satellite errors. Land cover was divided into developed, undeveloped and open water. Developed land constitutes roads, buildings, pavements parking lots and other impervious surfaces. Undeveloped land includes bare soil, agricultural land, forest, etc. Open water refers all kinds of water bodies. Figure 4.3 shows LULC change of the two decades studied. The trend of LULC change from 1991 to 2011 is also illustrated in Figure 4.4.

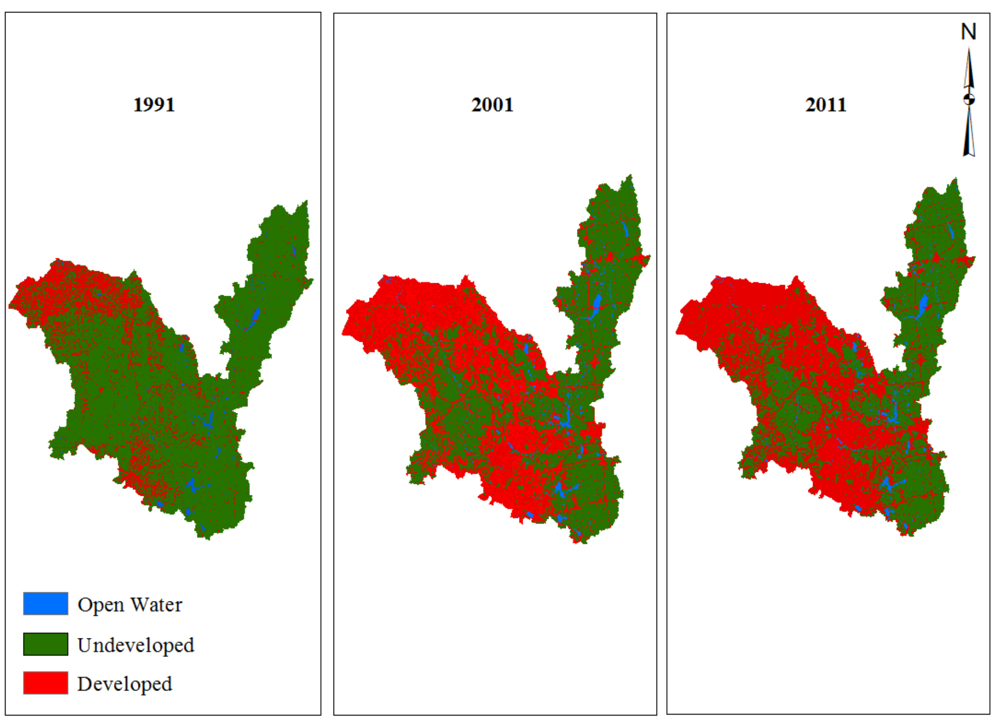

4.3: LULC Change for 1991,2001 and 2011

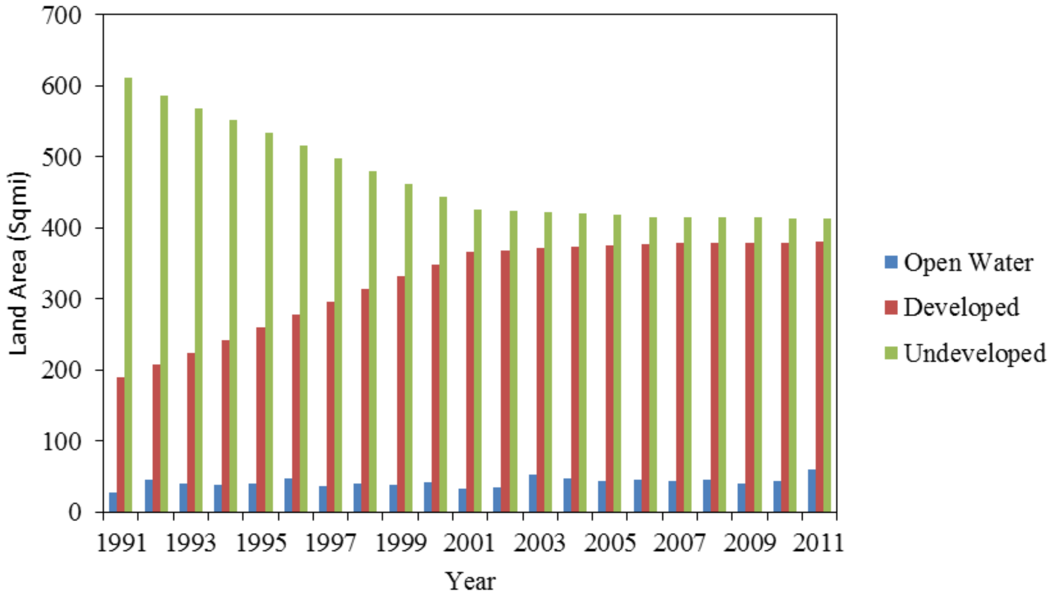

4.4: LULC Change for 1991,2001 and 2011

Table 4.4 and Table 4.5 list the parameters and test statistics obtained from the multiple linear regression. The magnitude of these coefficients (slopes) measures the degree to which the response (annual mean Suspended Sediment Load) is affected by a unit change in the predictor variable. To that end, one unit increase in total annual precipitation results in an additional 38.54Ton/day of SSL while a unit increase in developed land contributes an additional 0.85Ton/day of SSL. Figure 4.5 illustrates a comparison of the predicted annual mean SSL with the observed values at the Independence gage station.

Table 4. 4: Model Parameters

Variable	Description	Value	95% lower Conf. bound of β	95% Upper Conf. bound of β
α	Intercept	-915.99	-1824.5	-7.45
β_1	Slope (Annual PRCP)	38.54	16.89	60.19
β_2	Slope (Dev. Area)	0.85	-1.29	2.99

Table 4. 5: Test Statistics

	Statistic			
	R-Square	F-Statistic	P-Value	Err. Var.
Value	0.49	8.69	0.0023	83181

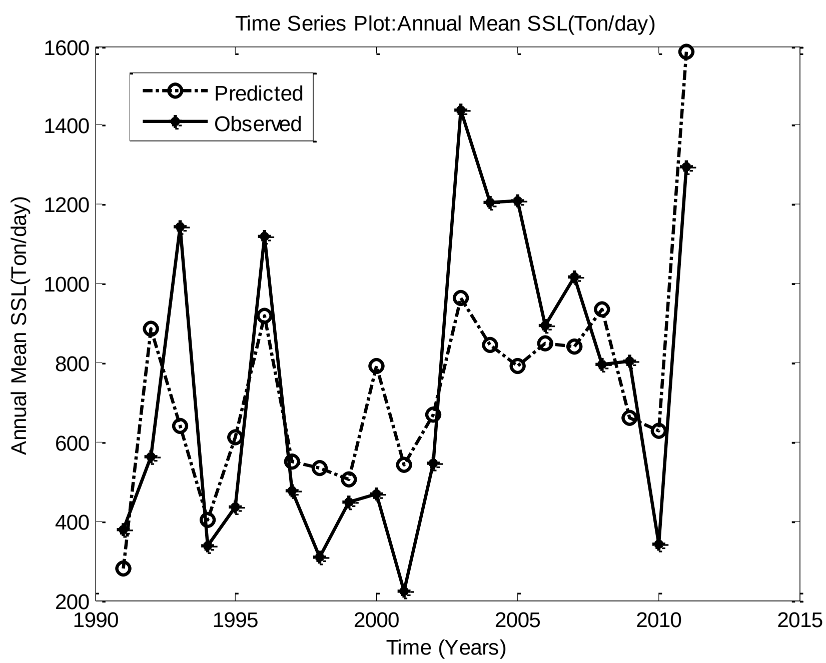

Figure 4. 5: Comparison of Predicted Annual Mean SSL with Observed

The computed R-square of 49 percent (Table 4.5) indicates that there may be other variables contributing to the annual mean SSL which are not included in the model. This may also account for the over-predictive and under-predictive nature of the model results (Figure 4.5) since the expected SSL was computed using only the LULC and precipitation.

At a 95% confidence level, the P-value (Table 4.5) for the F-statistic is significant. The regression model therefore confirms a significant impact of precipitation and LULC change on SSL from the Cuyahoga Watershed.

4.3 Assessing the contribution of each variable

The semi-partial correlation coefficient also known as the part correlation is commonly applied in multiple linear regression to study the portion of the variance contributed by each independent variable or the unique contribution of each predictor on the response variable after all the other predictors are controlled for (Ley, 1972; Tabachnick and Fidell, 1996). The semi-partial correlation coefficient between LULC and SSL after controlling for PRCP is given as:

$$r_{SSL(LULC,PRCP)} = \frac{r_{SSL.LULC} - r_{SSL.PRCP}r_{LULC.PRCP}}{\sqrt{1 - r_{LULC.PRCP}^2}}$$

Similarly, the semi-partial correlation coefficient between PRCP and SSL after controlling of the LULC is given as:

$$r_{SSL(PRCP,LULC)} = \frac{r_{SSL.PRCP} - r_{SSL.LULC}r_{PRCP.LULC}}{\sqrt{1 - r_{PRCP.LULC}^2}}$$

The correlation coefficient between SSL and LULC ($r_{SSL.LULC}$) is computed as 0.31, $r_{PRCP.SSL}$ is computed as 0.69 and $r_{LULC.PRCP}$ is computed as 0.25. Then, the semi-partial correlation coefficients $r_{SSL(LULC,PRCP)}$ and $r_{SSL(PRCP,LULC)}$ are computed as 0.14 and 0.63 respectively. By comparing the sizes of the semi-partial correlation coefficients, it can be seen that the total annual precipitation has more contribution to the annual mean suspended sediment compared to the LULC.

4.4 Validation of Assumptions for Multiple Linear Regression

Similar to the simple linear regression, multiple linear regression has four underlying assumption of the model residuals ($\boldsymbol{e}$) that must be satisfied for the model to be valid (Freund and Wilson, 1998): (1) $\boldsymbol{e}$ follow normal distribution; (2) $\boldsymbol{e}$ have a mean of zero; (3) $\boldsymbol{e}$ have the same variance and (4) $\boldsymbol{e}$ are random and independent. One may also summarize the above four assumptions as: $\boldsymbol{e}$ is I.I.D. random variable belonging to white Gaussian noise, i.e., $e \sim N(0, \sigma_e^2)$.

Graphically, the Q-Q plot in Figure 4.6 confirms the model residuals may be successfully modeled with a normal distribution and the histogram in Figure 4.7 shows that the model residuals may follow the Gaussian distribution. The assumptions of white Gaussian noise are therefore satisfied. And to this end, it is valid to apply the MLR model in the study.

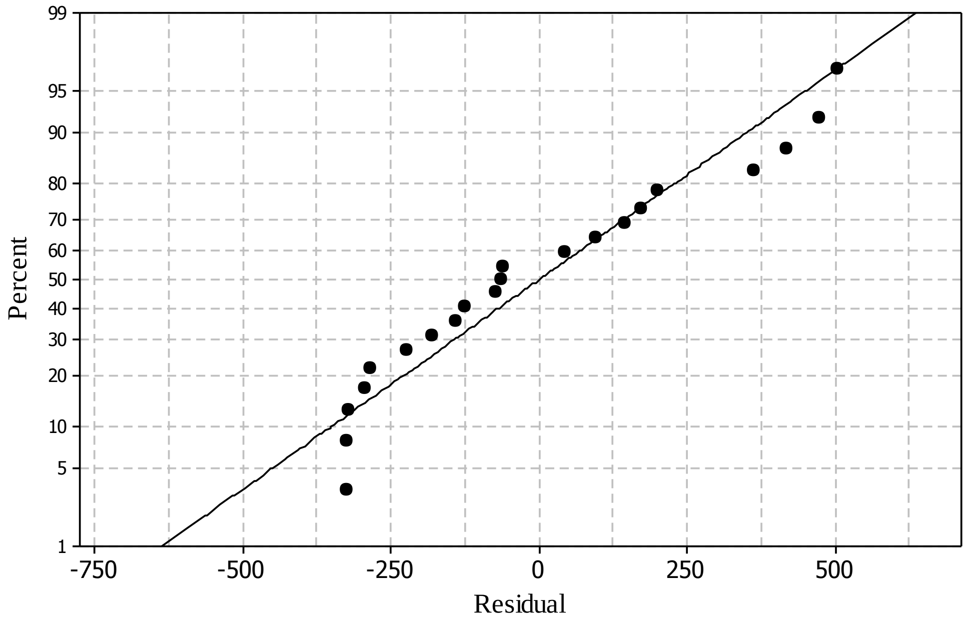

Figure 4. 6 : Q-Q Plot of Residuals

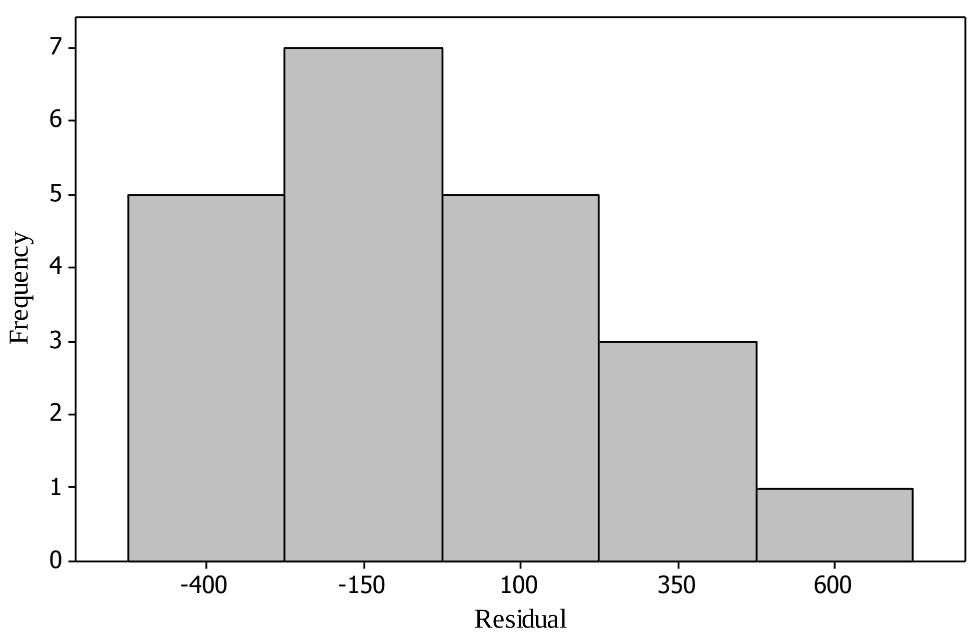

Figure 4. 7: Histogram of Model Residuals

CHAPTER V

CONCLUSIONS AND RECOMMENDATIONS

According to the objectives of this study (1) to project the annual harvestable sediment from the Cuyahoga River and perform a benefit cost analysis of using the harvested sediment for beneficial purposes and (2) to establish the impact of climate, land use and land cover change on the suspended sediment load of the Cuyahoga River over the past two decades, the study results in the following conclusions and recommendations.

5.1 Conclusions

Most of the organic and inorganic contaminants in the bedload sediment are below OEPA allowable concentrations which makes havested sediment suitable for beneficial use. The study found a projected harvestable annual sediment amount of 71,226.01 CY (89,513.77 Ton) using a sediment trap. The benefit-cost ratio (B/C) for installing sediment trap to harvest sediment for beneficial use is 1.69. This indicates that harvesting of sediment for commercial use is profitable. The study also reveals that sediment harvesting will be more beneficial than dredging sediment to CDFs.

A probabilistic model has been developed to investigate the impacts of climate and LULC change on sediment transported in the Cuyahoga River.

The analyses of climate and LULC change over the past two decades show a significant impact on suspended sediment in the river. Remote sensing analysis reveals that developed LULC change in the first 10 years (1991 to 2001) was more rapid (23% to 45%) than the last 10years (45% to 47%). Overall, developed land area doubled over the past two decades.

5.2 Recommendations

1. A more detailed study, including all hydraulic structures such as dams, bridges that may impact sediment yield, should be carried out for an improved result.
2. The proposed design of a sediment trap should consider the projected harvestable sediment size range of 0.125mm (very fine sand) to 8mm (fine gravel).
3. Although harvesting of sediment for commercial use is found to be viable, further studies should be carried out to ascertain the market preference for harvested sediment.
4. Future land developments in the Cuyahoga Watershed should be considered for the long term impact on sediment accumulation in the Cuyahoga River.
5. The next phase of this study is to model the response of the total annual harvestable sediment to LULC and climate change. This may be used in assessing the long-term sustainability of the sediment harvesting project.

REFERENCES

Abernethy, C. (1990). The use of river and reservoir sediment data for study of regional soil erosion rates and trends. *International Symposium on Water Erosion.* Dehradun, India.

Abrahams, A. D., & Parsons, A. J. (1991). Relation between sediment yield and gradient in debris covered hillslopes, Walnut Gulch, Arizona. *Geological Soceity of America Bulletin, v. 103*, 1109-1113.

Ackers, P., & White, W. R. (1973). Sediment Transport: New Approach and Analysis. *Journal of the Hydraulics Division*.

Alalandco(2013). Retrieved from http://www.alalandco.com/or2/index.php?action=listingview&listingID=1555

Area Mulch and Soils. (2014). Retrieved from http://www.areamulchandsoils.com/price%20list%20gravels.html

Ariathurai, R., & Krone, R. B. (1976). Finite element model for cohesive sediment transport. *J. of the Hydr. Div. ASCE,*, 102(HY3).

Bagnold, R. A. (1977). Bed load trasport by natural rivers. *Water Resources Research 13(2)*, 303-312.

Baker, M. D. (2011). *National Center for Water Quality Research*. Retrieved from Tributary Data: http://www.heidelberg.edu/academiclife/distinctive/ncwqr/data.

Betrie, G. D., van Griensven, A., Mohamed, Y. A., Popescu, I., Mynett, A., & Hummel, S. (2011). Linking SWAT and SOBEK using open modelling interface(OpenMI) for sediment transport simulation in the Blue Nile River basin. *Trans. ASABE*, 54(5), 1749-175.

Brunner, G. W. (2010). *HEC- RAS River Anlysis System Hydraulic Reference Manual.*

Canty, M. (2007). *Image Analysis, Classification, and Change Detection in Remote Sensing, with Algorithms for ENVI/IDL.* Boca Raton,FL: CRC Press.

Case Western Reserve University. (1998). CUYAHOGA RIVER . *The Encyclopedia of Cleveland History*. Retrieved from http://ech.case.edu/ech-cgi/article.pl?id=CR9

Casulli, V., & Zanolli, P. (2002). Semi-implicit numerical modelling of non-hydrostatic free surface flows for environmental problems. *Mathematical and Computer Modelling 36*, 1131-1149.

Casulli, V., & Zanolli, P. (2005). High resolution method for multidimensional model based on the shallow water equations. *International Journal for Numerical Methods in Fluids 32*, 331-348.

Chow, V. T. (1959). *Open Channel Hydraulics.* NY: McGraw-Hill Book Company.

Dearing, J. A., & Jones, R. T. (2003). Coupling temporal and spatial dimensions of global sediment flux through lake and marine sediment records. *Glob.Planet.Change 39*, 147-168.

Dendy, F. E., Champion, W. A., & Wilson, R. B. (1973). Reservoir sedimentation surveys in the United States. *American Geophyisical Union Monograph*, 349-357.

Duirk, S., & Gnap, A. (2013). *Cuyahoga River Sediment Sampling, Stage 3: Final Report on Bedload Sediment Contaminants Sampling.* Akron,OH.

Eco Reclamation. (2007). *Eco Reclamation Benefits*. Retrieved from http://ecoreclamation.com/ecoreclamation_benefits.html

Edwards, K. (1987). *Runoff and soil loss studies in New South Wales.* No. 10 Sydney NSW , Australia.: Soil Conservation Service of NSW, and Macquarie Univeristy Technical Handbook.

Einstein, A. H. (1950). *The Bed- Load Function for Sediment Transportation in Open Channel Flows.* Washington, D. C.: United States Department of Agriculture.Soil Conservation Service.

Engelund, F., & Hansen, E. (1967). *A Monograph on Sediment Transport in Alluvial Stream, 1-63.* Teknisk Forlag: Copenhagen V, Denmark.

Evans, J. B., Wass, P. D., & Hodgson, P. (1997). Integrated continuous water quality monitoring for the LOIS River syndrome. *Science of the Total Environment*, 194(195), 137-146.

Fernandez-Nieto, E. D., Lucas, C., Morales de Luna, T., & Cordier, S. (2014). On the influence of the thickness of the sediment moving layer in the definition of the bedload transport formula in Exner systems. *Computers & Fluids 91*, 87-106.

Freund, R. J., & Wilson, W. J. (1998). *Regression Analysis: Statistical Modeling of a Response Variable.* San Diego USA and London UK: Academic Press.

Gilbert, G. K. (1980). *Geology of the Henry Mountains: U.S. Geographical and Geological Survey of the Rocky Mountain Region Report.* 170p.

Griensven, A. v., Popescu, I., Abdelhamid, M. R., Preksedis, N. M., Lindsay, B., & Getnet, B. D. (2013). Comparison of sediment transport computations using hydrodynamic versus hydrologic models in the Simiyu River in Tanzania. *Physics and Chemistry of the Earth*, 61-62 (2013) 12-21.

Hammer, T. R. (1972). Stream channel enlargement due to urbanization. *Water Resources Research 8*, 1530-1540.

Henderson, F. M. (1966). Open-Channel Flow. New York: Macmillan Co.

http://www.geotechnicalinfo.com/soil_unit_weight.html. (n.d.). *GeotechnicalInfo*.

Huang, J. V., & Greimann, B. (2007). *User's Manual for SRH-1D V2.0(Sedimentation and River Hydraulics -One Dimension, Version 2.0).* Denver, Colorado.: Technical Service Center, U.S. Bureau of Reclamation.

Hull & Associates Inc ; Moffatt & Nichol. (2012). *Sediment Characterization And Yield Sustainable Sediment Management : Dredging Projections and Alternative Analysis draft report.*

Hull & Associates Inc. & Moffat & Nichol. (2012). *Sediment Characterization and Yield Sustainable Sediment Management ; Numerical Modeling of Existing Conditions Draft Report.*

Hydrologic Engineering Center. (1991). *HEC-2, Water Surface Profiles, User's Manual.* Davis CA.: U.S.Army Corps of Engineers.

IPCC. (2007). Climate change 2007:the physical basis. In S. Solomon, D. Qin, M. Manning, Z. Chen, K. Averyt, M. Tignor, & H. Miller, *Contribution of Working Group I to the Fourth Assessment Report of the Intergovernmental Panel on Climate Change.* Cambridge, United Kindom and New York, USA., Cambridge,, United Kindom: Cambridge University Press.

Jansen, P., & Bendegon, L. (1979). *Principle of River Engineering. Delftse.* Maatschappij, Delft.: Delftse Uitgevers.

Jansson, M. B. (1988). A global survey of sediment yield. *Geografiska Annaler Series A Physical Georgraphy*, 70,81-89.

Jensen, J. R. (2005). *Introductory Digital Image Processing: A Remote Sensing Perspective 3rd Edition.* Upper Saddle River,NJ: Pearson Prentice Hall.

Kirbysand. (2014). Retrieved from http://www.kirbysand.com/blank?pageid=8&catstart=0&prodstart=0

Kreitinger, J. P., Price, R. A., Borrowman, T. D., Kennedy, J. A., & Michelle, B. (2011). *Evaluation of Beneficial Use Suitabililty for Cleveland Habor Dredged Material: Interim Capacity Management and Long-Term Planning.* ERDC/ELTR-11##, US Army Research and Development Center,Vicksburg ,MS.

Krone, R. B. (1962). *Flume Studies of the Transport of Sediment In Estaurial Shoaling Processes, Final Report.* University of California, Berkeley.

LandWatch. (2014). Retrieved from http://www.landwatch.com/Bell-County-Kentucky-Land-for-sale/pid/204501287

Lapuszek, M., & Paquier, A. (2008). Practical Application of 1-D Sediment Transport Model. *Archives of Hydro- Engineering and Environmental Mechanics Vol. 54 (2007) , No. 4,* pp. 245-260.

Leopold, L. B. (1968). Hydrology for urban land planning; a guidebook on the hydrologic effects of urban land use. *USGS Circular 554*, 18p.

Ley, P. (1972). Quantitative Aspects of Psychological Assessment. Duckworth: London.

Lillesand, T. M., & Keiger, R. W. (2008). *Remote Sensing and Image Interpretaton.* NY: John Wiley and Sons, Inc.

McBean, G., & Ajibade, I. (2009). Climate related hazards and human settlements. . *Current Opinion in Environmental Sustainability 1 (2)*, 179-186.

Meade, R. H., & Parker, R. S. (1984). Sediment in rivers of the United states. *U.S. Geological Survery Water Supply Paper no. 2275*, 49 -60.

Methods, H., Dyhouse, G., Hatchett, J., & Benn, J. (2003). *Floodplain Modeling using HEC-RAS.* Wasterbury,CT: Haestad Press.

Meyer- Peter E, M. R. (1984). Formulas for bed transport. *Report on second meeting of IAHR,Stockholm*, 39-64.

Miche, G. R. (2001). Net Present Value Analysis:A Primer for Finance Officers. *Government Finance Review*, pp. 27-31.

Miller, P. D., & Komar, M. C. (1973). Journal of Sediment movement under oscillatory water waves. *Journal of Sedimentary Petrology 43(4)*, 1101-1110.

Minnesota Department of Transportation. (2012). *Planning and Programming Benefit/Cost Analysis for Transportation Projects*. Retrieved from MnDoT Planning & Programming: http://www.dot.state.mn.us/planning/program/benefitcost.html

Molinas, A., & Yang, C. T. (1985). *Computer Program User's Manual for(GSTARS) Generalized Stream Tube model for Alluvial River Simulation.* U.S. Bureau of Reclamation, Denver, Colorado, November.

Molinas, A., & Yang, C. T. (1985). Generalized Water Surface Profile Compuation. *ASCE Journal of Hydraulic Engineering, Vol. 111, No. 3,*, 381-387.

Nelson, E. J., & Booth, D. B. (2002). Sediment sources in an urbanizing, mixed land-use watershed. *Journal of Hydrology*, 51-68.

Newson, M. D. (1986). River basin engineering. Fluvial geomorphology. *Journal of the Instituion of Water Engineers and Scientist*, 40 (4) ,307-324.

North Ohio Regional Sewer District. (2014). *Southerly Wastewater Treatment Plant*. Retrieved from http://www.neorsd.org/southerly.php?a=read_more

Novotny, V., & Olem, H. (1994). Water Quality: Prevention, Identification and Management of Diffuse Pollution. New York: Van Nostrand Reinhold.

Odhiambo, B. K., & Boss, S. K. (2006). Watershed Physiography, Land Use, and Sediment Yield: A Case Study from Northwest Arkansas. *Journal of Spatial Hydrology*.

Ohio department of taxation. (2014). *Annual Certified Interest rates*. Retrieved from http://www.tax.ohio.gov/ohio_individual/individual/interest_rates.aspx

Olive, L. J., & Rieger, W. A. (1984). Sediment erosion and transport modeling in Australia. In T. a. Drainage Basin Erosion, *A conference on Erosion, Transportation and Sedimentation* (pp. 81-91.). Newcastle, NSW,.

Paquier, A. (2003). What are the problems to be solved by a 1-D river sediment transport model? Example of RuberBE software. In *Selected Problems of Water Engineering, Politechnika Krakowska - Cemagref- results of cooperation* (pp. 75-85). Antony,France.

Parker, G. (1991). Selective Sorting and Abrasion of Rivers. *Journal of Hydraulic Engineering*, 131-147.

Parker, G., & Klingeman, P. C. (1982). On why gravel bed streams are paved. *Water Resources Research*, 18(5), 1409-1423.

Partheniades, E. (1962). *A Study of Erosion and Deposition of Cohesive Soils in Salt Water.* Berkeley PhD Dissertation.

Pemberton, E. L. (1980). Survey and prediction of sedimentation in reservoirs,. In H. Shen, & H. Kikkawa, *Application of Stochastic Processes in Sediment Transport: Water* (pp. 15,115,20). Littleton, Colo: Water Resources Publicatons.

Premier Equastrian. (2013). *Arena Sand Specifications.*

Rose, N. L., Morley, D., Appleby, P. G., Battarbee, R. W., Alliksaar, T., Guilizzoni, P., . . . Punning, J. (2011). Sediement accumulation rates in European lakes since AD 1850: trends, reference conditions and exceedence. *Journal of Paleolimnology 45*, 447-468.

Rubey, W. (1933). Settling velocities of gravel, sand, and silt particles. *Am. J. of Science*, 25.

Schiefer, E., Petticrew, E. L., Immell, R., Hassan, M. A., & Sonderegger, D. L. (2013). Land use and climate change impacts on lake sediment. *Anthropocene*, 61-71.

Smolen, M. D., Miller, D. W., Wyatt, L. C., Lichthardt, J., & Lanier, A. L. (1998). *Erosion and Sediment Control Planning and Design Manual.* Raleigh, NC.: North Carolina Sedimentation Control Commission; North Carolina Department of Environment, Health, and Natural Resources; and Division of Land Resources, Land Quality Section.

SWAN Team. (2009). *SWAN Scientific and Technical Documentation 40.72.* Delft University of Technology.

Tabachnick, G. B., & Fidell, S. L. (1996). In *Using Multivariate Statistics 3rd Edition* (pp. 127-192). HarperCollins College Publishers.

Tang, C., Crosby, B., Wheaton, J., & Piechota, T. C. (2012). Assesing streamflow sensitivity to temperature increases in the Salmon River Basin, Idaho. *Global and Planetry Change 88-89*, 32-44.

The Crooked River Project. (1997). *The Crooked River Project*. From http://www.grc.nasa.gov/WWW/k-12/fenlewis/Cuyahoga_River.html

Thomas, W. A. (1982). Gravel. In R. Hey, J. Bathrust, & C. R. Thorne, *Mathematical modeling of sediment movement* (p. Chapter 18). John Wiley & Sons Ltd.

Thothong, W., Sylvain, H., Jean-Louis, J., Arthorn, B., Anneke, d. R., Olivier, P., . . . Preeda, P. (2011). Impact of land use change and rainfall on sediment and carbon acculation in a water reservoir of North Thailand. *Agriculture, Ecosystems and Environment*, 521-533.

U. S. A. E. Water Experiment Station. (1988). *Report on IPA Activity, May-Dec 1988.* Vicksburg, MS.

U.S Geological Survery. (2009). *National Elevation Dataset.*

U.S Geological Survey. (1979). *Geographic Names Informatin System (GNIS)*. Retrieved from http://geonames.usgs.gov/pls/gnispublic/f?p=gnispq:3:3990939580975612::NO::P3_FID:1072205

U.S. Army Corps of Engineers. (2009). *Draft Cleveland Harbor Dredged Material Managment Plan and Environmental Impact Statement.*

U.S.G.S. (2013). *glovis*. Retrieved from http://glovis.usgs.gov/

USACE. (2004). *Cleveland Harbor, Ohio Dredged Material Management Plan Preliminary Assessment. Summary of Findings and Recommentations.*

USACE. (2006). *Beneficial Uses of Dredged Materials*. From http://el.erdc.usace.army.mil/dots/budm/intro.cfm?Topic=Intro

USACE. (2012). *Interim Dredged Material Plan and Environmental Assessment.* Buffalo District.

USACE, Hydrologic Engrg. Center. (1976). *HEC-2, Water Surface Profiles, Users Manual.*

USEPA. (2006, May 24). *Sediment Traps; Construction Site Stormwater Runoff Control*. Retrieved from USEPA.

USEPA. (2012, May 21). Sediment Traps ,CAG Meeting.

Van Dessel, W., Van Rompaey, A., Poelmans, L., & Szilassi, P. (2008). Predicting land cover changes and their impact on the . *Landscape Ecol. 23*, 645-656.

van Leussen, W. (1991). Sediment Transport under Tidal Action. *Geo-Marine Letters*, (pp. 119-126). Springer-Verlag, New York.

Van Rijn, L. C. (1984). Sediment Transport, part I:bed load transport. *Journal of Hydraulic Engineering*, 110(10) ,1431-1456.

Van, R., & Leo, C. (1993). Principles of Sediment Transport in Rivers, Estuaries,Coastal Seas and Oceans. *International Institute for Infrastructural, Hydraulic, and Environmental Engineering*. From http://www.acmesand.com/gravel/

Walling, D. E. (1999). Linking land use, erosion and sediment yields in river basins. *Hydrobiologia*, 233-240.

Walling, D. E., & Webb, B. W. (1986). Solutes in river systems. In S. Trudgill, *Solute Processes.* (pp. 251-320). Chichester: Wiley, John & Sons Ltd.

Wang, J., Ishidaira, H., & Zu, Z. X. (2012). Effects of climate change and human activities on inflow into the Hoabinh Reservoir in the Red River basin. *Procedia Environmental Sciences*, 1688–1698.

Webb, B. W., Foster, I. D., & Gurnell, A. M. (1995). Hydrology, water quality and sediment behavior. In I. Foster, A. Gurnell, & B. (. Webb, *Sediment and Water Quality in River Catchments* (pp. 1-30). Chichester: Wiley, John & Sons Ltd.

Wenatchee Sand & Gravel. (2014). *PRICING 2014*. Retrieved from http://www.wenatcheesandandgravel.com/core/files/wenatcheesandandgravel/uploads/files/2014%20WSG%20Gravel%20Prices.pdf

Westhook Sand and Gravel. (2014). Retrieved from http://westhooksandandgravel.com/Sand.html

Wolman, M. G. (1967). A cycle of sedimentation and erosion in urban river channels. *Geografiska Annaler 49A*, 385-395.

Wu, W., & Wang, S. S. (2006). Formulas for Sediment Porosity and Settling Velocity. *Journal of Hydraulic Engineering*, 858-862.

Yang, C. T. (1971). Potential energy and stream morphology. *Water Resources Research,AGU,7(2)*, 311-322.

Yang, C. T. (1976). Minimum unit stream power and fluvial hydrualics. *J. of the Hydr. Div. ASCE, 102(HY7)*, 919-934.

Yang, C. T. (1989, August). On Sediment Transport Modeling. *Proceedings of the International Symposium*, p. 653.

Yang, C. T., & Ahn, J. (2011). *Generalized Sediment Transport model for Alluvial River Simulation.* Hydroscience and Training Center, Colorado State University.

Yang, C. T., & and Song, C. C. (1986). Theory of minimum energy and energy dissipation rate. In N. (. Cheremisinoff, *Encyclopedia of Fluid Mechanics, Vol. 1,Chapter 11* (pp. 353-399). Gulf Publishing Company.

Yang, C. T., & Simoes, F. J. (2000). *User's manual for GSTARS 2.1(Generalized Stream Tube model for Alluvial River Simulation version 2.1).* Denver, Co.: U.S. Bureau of Reclamation, Technical Service Center.

Yang, C. T., & Somoes, F. J. (2002). *User's Manual for GSTARS3 (Generalized Sediment Transport model for Alluvial River Simulation version 3.0).* Denver,CO.: U.S. Buearu of Reclamation, Technical Service Center.

Yang, C. T., & Song, C. C. (1979). Theory of minimum rate of energy dissipation. *J. of the Hydr. Div. ASCE 105(HY7)*, 769-784.

APPENDICES

APPENDIX A

SEDIMENT TRANSPORT FUNCTION SELECTION

Function	d	d_m	s	V	D	S	W	T
Ackers-White (*flume*)	0.04 - 7.0	NA	1.0 - 2.7	0.07 - 7.1	0.01 - 1.4	0.00006 - 0.037	0.23 - 4.0	46 - 89
Englund-Hansen (*flume*)	NA	0.19 - 0.93	NA	0.65 – 6.34	0.19 – 1.33	0.000055 – 0.019	NA	45 - 93
Laursen (*field*)	NA	0.08– 0.7	NA	0.068 – 7.8	0.67 – 54	0.0000021 – 0.0018	63 – 3640	32 - 93
Laursen (*flume*)	NA	0.011 - 29	NA	0.7 - 9.4	0.03 – 3.6	0.00025 – 0.025	0.25 – 6.6	46 - 83
Meyer-Peter Muller (*flume*)	0.4 – 29	NA	1.25 – 4.0	1.2 – 9.4	0.03 – 3.9	0.0004 – 0.02	0.5 – 6.6	NA
Tofaletti (*field*)	0.062 – 4.0	0.095 – 0.76	NA	0.7 - 7.8	0.07 – 56.7 (R)	0.000002 – 0.0011	63 - 3640	32 – 93
Tofaletti (*flume*)	0.062 – 4.0	0.45 – 0.91	NA	0.7 - 6.3	0.07 – 1.1 (R)	0.00014 – 0.019	0.8 – 8	40 - 93
Yang (*field-sand*)	0.15 – 1.7	NA	NA	0.8 - 6.4	0.04 – 50	0.000043 – 0.028	0.44 – 1750	32 - 94
Yang (*field-gravel*)	2.5 – 7.0	NA	NA	1.4 - 5.1	0.08 – 0.72	0.0012 – 0.029	0.44 – 1750	32 - 94

Where: d = Overall particle diameter, mm

d_m = Median particle diameter, mm

s = Sediment specific gravity

V = Average channel velocity, fps

D = Channel depth, ft

S = Energy gradient

W = Channel width, ft

T = Water temperature, °F

(R) = Hydraulic Radius, ft

NA = Data not available

APPENDIX B

PARTICLE SIZE CLASSIFICATION BY THE AMERICAN GEOPHYSICAL UNION

Sediment Material	Grain Diameter Range(mm)	Geometric Median Diameter (mm)
Clay	0.002-0.004	0.003
Very Fine Silt	0.004-0.008	0.006
Fine Silt	0.008-0.016	0.011
Medium Silt	0.016-0.032	0.023
Coarse Silt	0.032-0.0625	0.045
Very Fine Sand	0.0625-0.125	0.088
Fine Sand	0.125-0.250	0.177
Medium Sand	0.250-0.5	0.354
Coarse Sand	0.5-1.0	0.707
Very Coarse Sand	1-2	1.41
Very Fine Gravel	2-4	2.83
Fine Gravel	4-8	5.66
Medium Gravel	8-16	11.3
Coarse Gravel	16-32	22.6
Very Coarse Gravel	32-64	45.3
Small Cobbles	64-128	90.5
Large Cobbles	128-256	181
Small Boulders	256-512	362
Medium Boulders	512-1024	724
Large Boulders	1024-2048	1448

APPENDIX C

SAMPLE EXCESSIVELY CLOUDED IMAGE

APPENDIX D

SAMPLE CLASSIFIED IMAGE (BEFORE MASKING OF CLOUD)

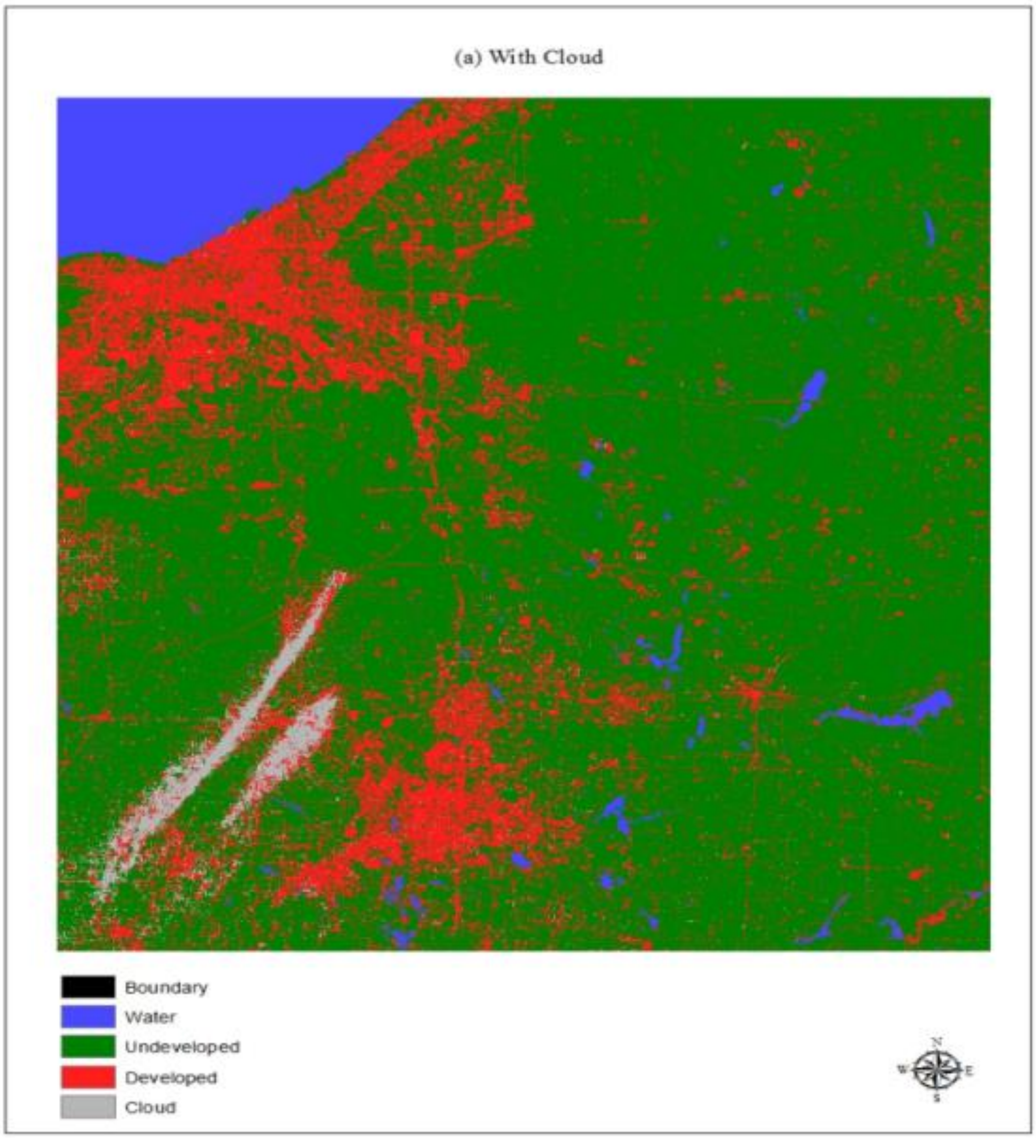

APPENDIX E

SAMPLE CLASSIFIED IMAGE (AFTER MASKING OF CLOUD)

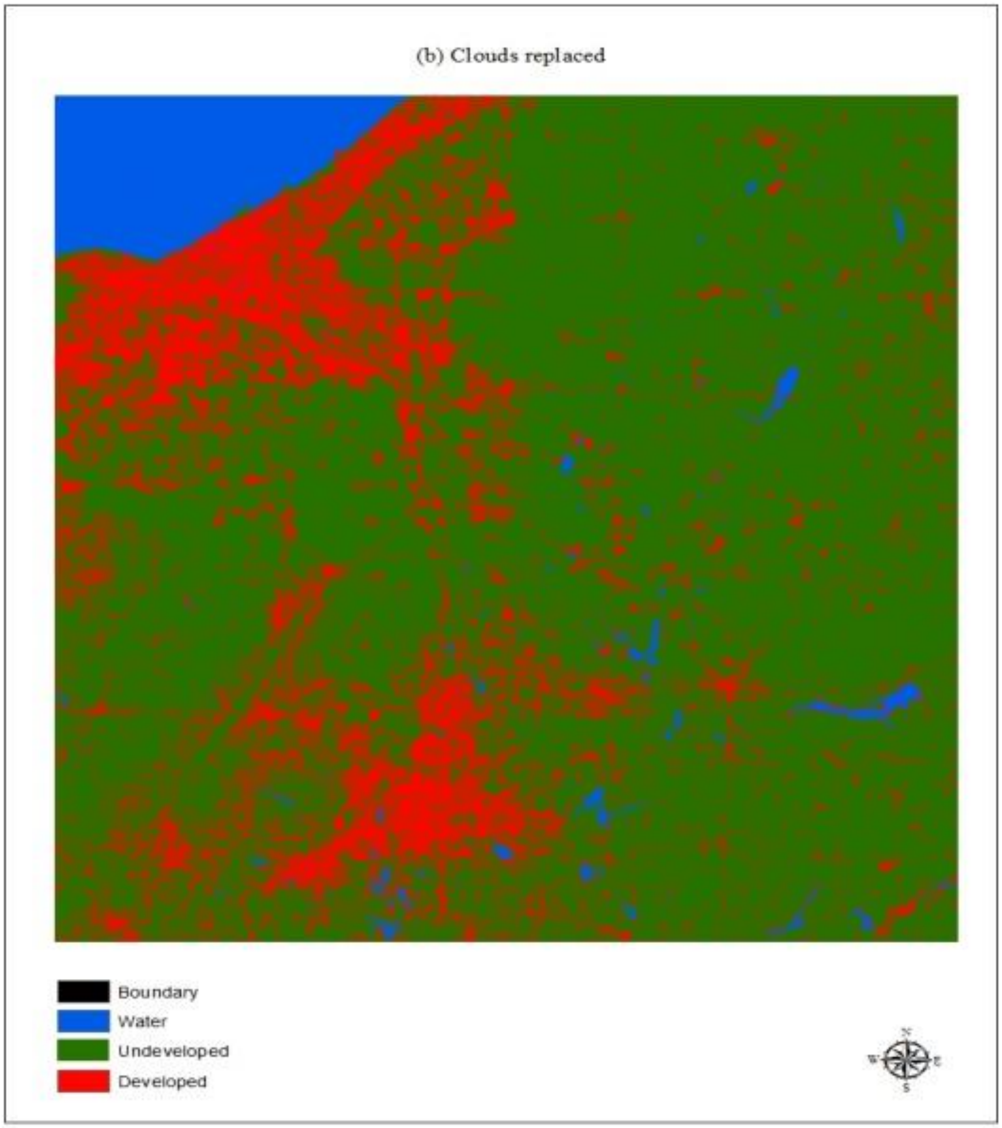

APPENDIX F

TOTAL ANNUAL PRECIPITATION AVERAGED BY THE THIESSEN POLYGON

	Weather Station and Percentage of Area Contributed					
Year	Akron-Canton (in) 10.18%	Ravena (in) 57.01%	Harim (in) 14.28%	Chippewa (in) 6.61%	Chardon (in) 11.91%	Thiessen Weighted Average Precipitation (in)
1991	24.08	32.67	29.83	22.46	34.32	26.82
1992	45.14	48.53	49.03	44.17	50.06	42.19
1993	41.23	40.63	39.24	37.26	44.17	35.43
1994	40.51	29.56	39.10	34.29	39.19	28.83
1995	35.65	39.05	39.18	36.92	46.22	33.93
1996	46.92	46.44	49.21	48.57	60.24	41.49
1997	32.29	35.36	39.07	38.17	47.27	31.55
1998	40.28	32.83	36.47	40.15	41.59	30.68
1999	35.81	31.97	38.36	33.64	47.95	29.58
2000	45.5	40.59	44.54	37.80	47.41	36.63
2001	32.86	34.38	35.12	27.44	36.97	29.78
2002	40.62	36.38	40.42	35.27	40.38	32.98
2003	51.10	42.50	55.97	48.00	55.50	40.60
2004	46.30	39.39	49.75	47.70	51.82	37.43
2005	41.17	39.87	43.76	42.84	54.37	36.01
2006	43.93	40.64	48.08	44.90	61.88	37.48
2007	40.89	41.44	46.48	43.00	58.40	37.27
2008	42.00	44.49	48.77	46.03	60.77	39.65
2009	35.61	35.76	42.16	37.84	47.60	32.54
2010	37.85	35.40	39.19	31.18	52.59	31.70
2011	58.37	65.32	66.13	59.27	53.06	56.55

APPENDIX G

COMPARISON OF HIGH, AVERAGE AND LOW FLOW

YEARS AT INDPENDENCE

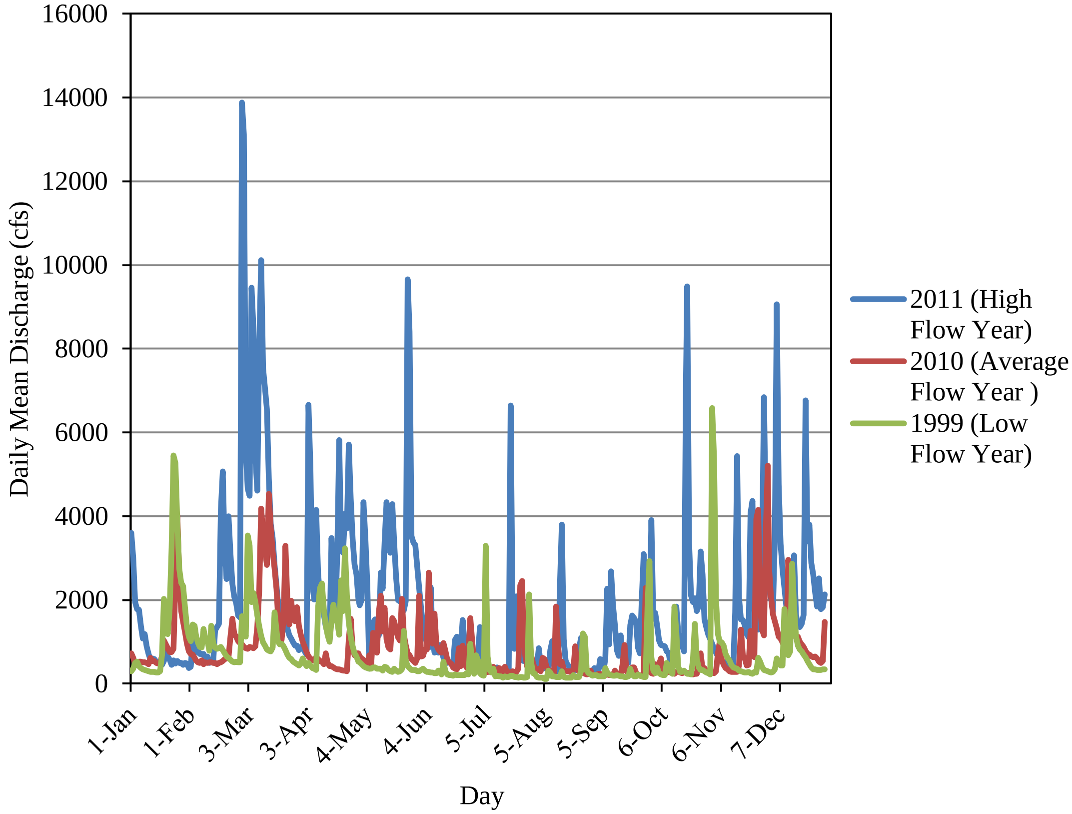

APPENDIX H

COMPARISON OF HIGH, AVERAGE AND LOW FLOW

YEARS AT OLD-PORTAGE

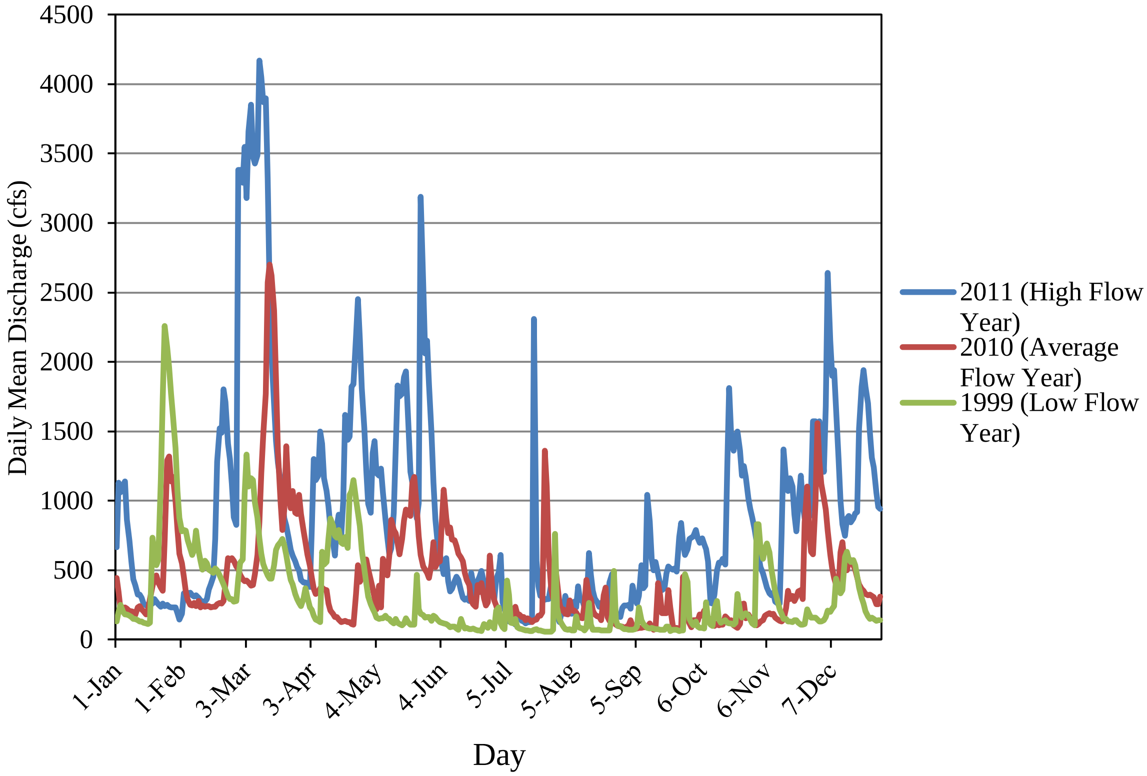

APPENDIX I

COMPARISON OF HIGH, AVERAGE AND LOW FLOW

YEARS AT HARIM RAPIDS

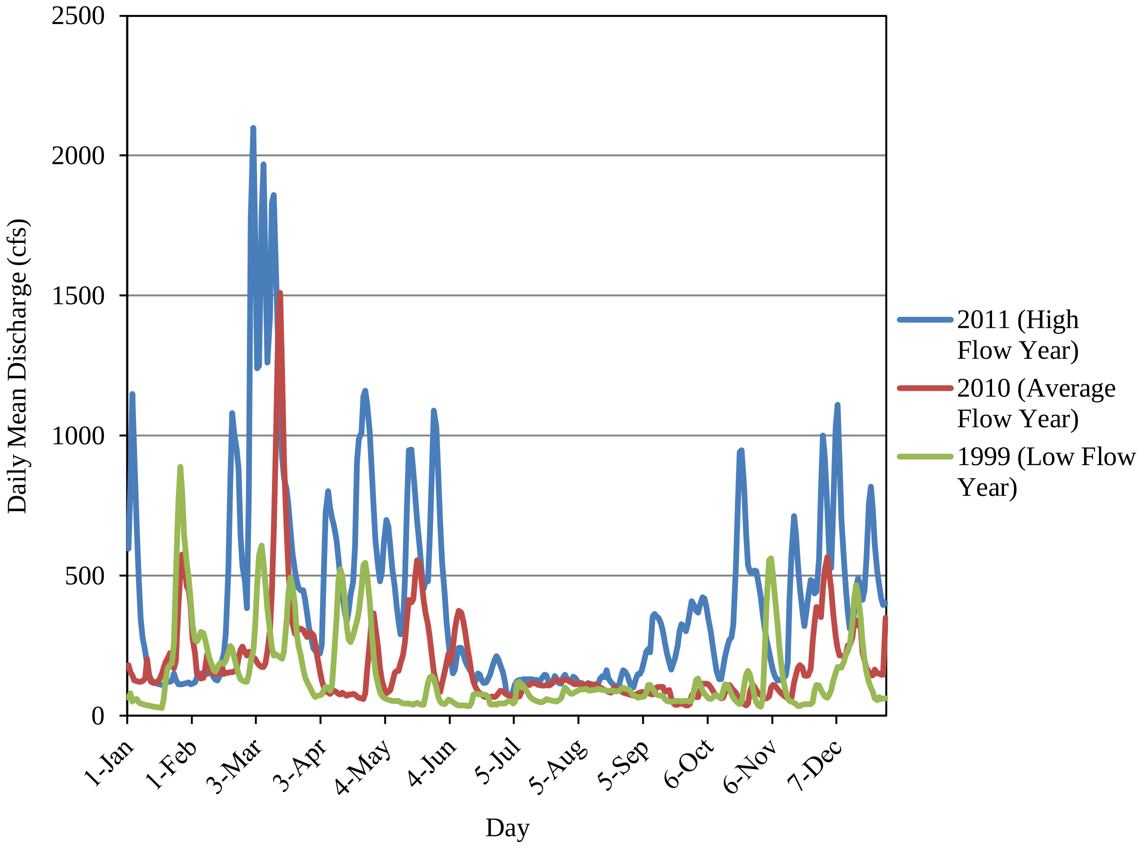

APPENDIX J

SUSPENDED SEDIMENT LOAD TIME SERIES AT INDEPENDENCE

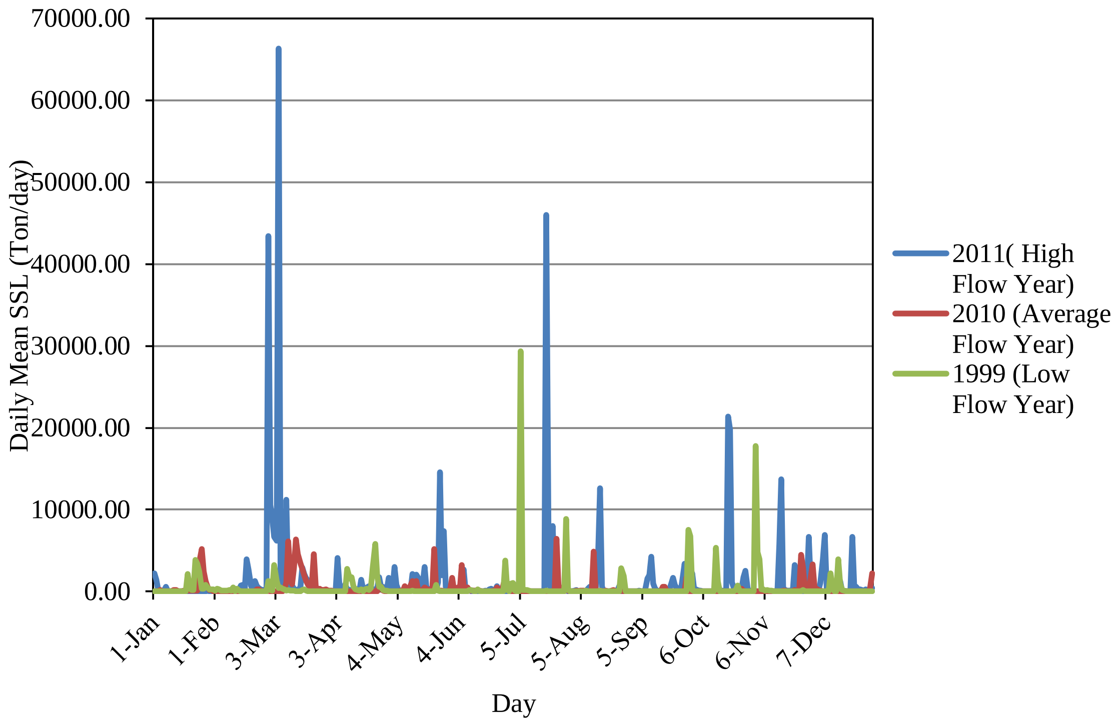

APPENDIX K

AVERAGE SHEAR VELOCITY AT NEWBURGH, BRADLEY ROAD AND INDEPENDENCE COMPARED WITH PARTICLE FALL VELOCITIES